COO-2229-2

RENSSELAER POLYTECHNIC INSTITUTE
Troy, New York 12181

31885

ANNUAL PROGRESS REPORT
(Covering the period 1 May 1972 - 31 January 1973)

under

CONTRACT NO. AT(11-1)-2229

entitled

ION BEAM PROBE PLASMA DIAGNOSTIC SYSTEM

Prepared by

R. L. Hickok, W. C. Jennings, G. S. Huchital, and R. E. Reinovsky

March 1973

DISCLAIMER

Abstract

The work covered in this report can be divided into four categories: (1) Cooperative effort with PPL to extract plasma current density distribution from beam probe measurements, (2) Design of beam probe system for Doublet II, (3) Design of beam probe system for United Aircraft Research Laboratory's "Baseball" device, and (4) Experimental program at RPI to measure T_e with ion beam probe. It is shown that the non-toroidal components of the CF field on the ST Tokamak rotated and demagnified the Z displacement of the secondary ions at the detector. Furthermore it is shown that this distortion can be subtracted out in the data reduction process. Preliminary design of a beam probe system for Doublet II, subject to the constraint of minimizing the entrance and exit ports, has been completed and shows that such a diagnostic system would permit measurements all along a line passing through the upper focal point. Considerable progress has been made on the design of a beam probe system for the UARL "Baseball" device. This design would permit measurements throughout a small volume near the center of the system using a single fixed detector. It has been shown that a two ion species beam probe system can be used to measure electron temperature in the range of 5 to 200 ev. Experimental verification at 7 ev has been obtained on the RPI hollow cathode discharge.

I. Introduction and Summary

This is the first annual progress report submitted under Contract AT(11-1)-229 covering the period May 1, 1972 to January 31, 1973. During this period the Principal Investigator, R. L. Hickok, Associate Professor, devoted approximately 1/3 of his time (25% during the academic year and 50% during 2 1/2 summer months) and faculty participant, W. C. Jennings, Assistant Professor, devoted approximately 1/3 of his time to this research program. (Only about 10% of Prof. Jennings time has been charged against the contract. The additional 23% of his time that he has devoted to this program has been donated by the university.) Both individuals will devote 1/4 of their time to this program during the remainder of the contract.

The principal objective of this program is the further development of ion beam probe diagnostic systems for magnetically confined high temperature plasmas. The research can be divided into three broad categories: (1) cooperation with Princeton Plasma Laboratory (PPL) on extracting the plasma current density from ion beam probe measurements on the ST Tokamak. (2) Preliminary design studies of ion beam probe systems for other major plasma devices supported by the AEC. (3) An in-house experimental program to improve and extend the measurements that can be made with an ion beam probe.

Principles of Beam Probing

An ion beam probe diagnostic system can provide a direct measurement of plasma density, space potential, current density and electron temperature. It provides 3 dimensional space resolution with a characteristic

dimension of a few mm, time resolution in the range of a few microseconds to a millisecond and the measurements are continuous in time. The range of plasma parameters that can be measured, the volume of plasma that can be sampled and the space and time resolution depend on the specific design of the beam probe system and the particular plasma device on which it is installed.

The basic physics of beam probing is quite simple. A singly charged ion beam is directed along a trajectory through the plasma and some of the beam ions make ionizing collisions with the plasma electrons to form doubly charged ions. Since the momentum of the ions in the primary beam is an order of magnitude larger than the momentum of the electrons, there is essentially no momentum transfer in the collision. Consequently the secondary, or doubly charged, ions are created with the same momentum as the ions of the primary probing beam, but will be separated from the primary beam since they have half the radius of curvature in the confining magnetic field. Secondary ions will be created all along the primary trajectory but the secondaries from each point on the primary trajectory will follow a distinct path that is completely determined by the magnetic field. A small detector placed to intercept the secondaries from some point x on the primary trajectory will only look at a small volume of plasma centered at x. This volume (the spatial resolution) is determined by the size of the detector, the size of the beam and the magnetic field geometry. A simplified sketch of the basic operation of beam probing is shown in Fig. I-1.

The ratio of the secondary current intensity at the detector to the intensity of the primary beam, I_s/I_p, is a measure of $n_e F(T_e)$ at x.

Beam Probe Operation

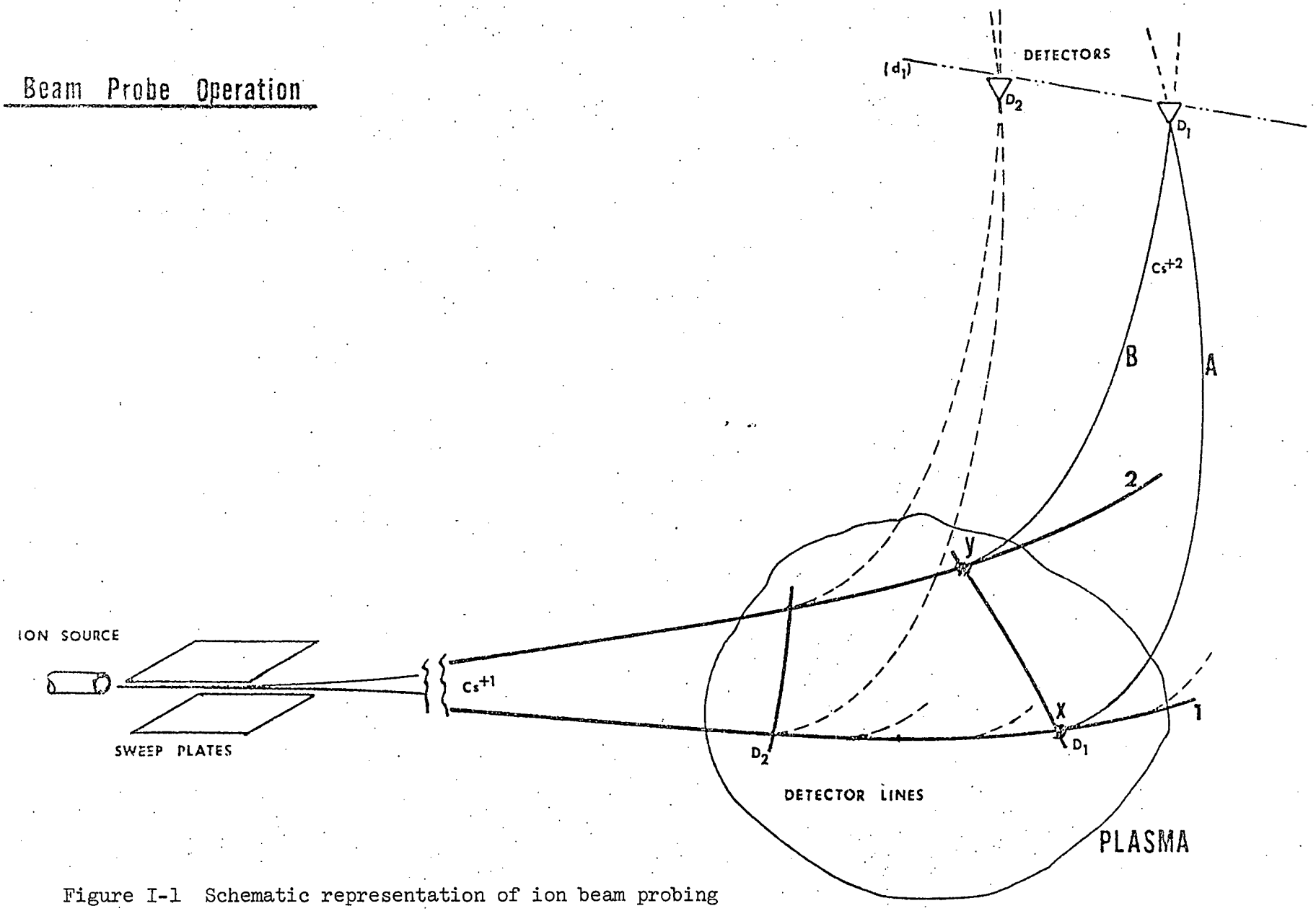

Figure I-1 Schematic representation of ion beam probing

n_e is the plasma electron density and $F(T_e)$ is a function of the electron temperature that depends on the 1^+ to 2^+ effective ionization cross section for the particular ion species being used. If measurements are made with two different ion species that have different cross sections, then n_e and T_e can both be evaluated.

$$\frac{I_{s_1}/I_{p_1}}{I_{s_2}/I_{p_2}} = \frac{n_e F_1(T_e)}{n_e F_2(T_e)} = \frac{F_1(T_e)}{F_2(T_e)}$$

The function $F(T_e)$ is equal to σv averaged over the electron velocity distribution taking into account the finite velocity of the ion beam. Once the temperature has been evaluated the density can be determined from I_s/I_p for either ion species.

Initial energy of the primary ion is eV_{acc}, where V_{acc} is the accelerator voltage of the primary injection system. At x it has the energy $e(V_{acc} - \phi)$ where ϕ is the space potential. The secondary ion gains $2e\phi$ in going from x to the detector, so the final energy of the secondary ion is $e(V_{acc} + \phi)$. This can be measured to an accuracy of approximately 10^{-4} V_{acc} and provides a direct evaluation of the space potential at x.

The trajectories for both the primary and secondary beams are principally determined by the vacuum magnetic field produced by current flow in external windings. If there is current flow in the plasma it will produce a magnetic field that will distort the zero order beam trajectories. Generally it is possible to measure this distortion and use the results to evaluate the plasma current density distribution. This evaluation is not necessarily unique and the ability to extract the current density must be evaluated for each specific installation.

Summary of Results Obtained During the Contract Period 1 May 1972 - 31 January 1973

The primary complication in extracting the plasma current density from beam probe measurements on the ST Tokamak is correcting for the z displacement of the beam by the non-toroidal components of the confining field (fringing field effect). Detailed computer calculations of the ion trajectories has shown that the fringing fields produce a rotation of the experimentally measured Z_D versus R_e curve and a demagnification of the Z displacement. To first order both of these effects are independent of the current density distribution. Extraction of the current density requires double differentiation of the experimental curve. Consequently, the rotational correction drops out in the data processing and the demagnification affects the absolute value of the current density but does not distort the shape of the distribution.

Preliminary design of an ion beam probe system for Doublet II has been completed. The design minimizes the port requirements but would provide detailed measurements along a single primary ion trajectory. This trajectory has an average angle of 45° with the horizontal and passes through the upper focal point on Doublet II. This system would provide density, electron temperature, space potential, and current density measurements at any point along this trajectory with a spatial resolution of the order of 0.1 cm^3. Simultaneous measurements could be made at any number of points by use of multiple detectors. Time resolution for n, ϕ, and J(r) would be less than 100 μsec and for T_e it would be of the order of 1 msec.

A preliminary design study of an ion beam probe system for the "baseball" device at the United Aircraft Research Laboratory is being actively pursued. Initial results indicate that the entrance and exit ports should be diametrical opposite one another with an angular separation between the incident primary and the exiting secondary beams of the order of 30^{o}. By sweeping the 2 angular directions of the beam and the beam energy it should be possible to map a plasma volume of the order of 100 cm^3 in the neighborhood of the center of the system. In contrast with the Doublet II system the "baseball" beam probe would only use one fixed detector and the mapping would be performed by sweeping the primary beam. Space and time resolution would be about the same as for Doublet II.

Beam probe measurements on the RPI hollow cathode discharge (HCD) have clearly demonstrated that ion beam probing can be used to measure electron temperature for low temperature systems (less than 200 ev). By using two ion beams we have measured radial profiles of T_e and n on the HCD. T_e is the order of 7 ev and the accuracy of the measurement is better than 10%. The error in the abolute density measurement is quite large since the two ion species were chosen to maximize the sensitivity to T_e.

II. Plasma Current Density on the ST Tokamak

Our cooperative program with the Princeton Plasma Laboratory is concerned primarily with understanding the problems associated with extracting the plasma current density from the measured displacements of the secondary ions. It has previously been shown that for a pure cylindrical system where the confining magnetic field (CF) has only a Z component and the plasma current is only in the Z direction, the Z displacement of the secondary ion beam can be analytical related to plasma current density at the creation point of the secondary ion. Specifically it has been shown that

$$\frac{d \dot{Z}_D}{d r_e} = K B_\theta (r_e)$$

and

$$\frac{d Z_D}{d r_e} = K' B_\theta (r_e) + (\text{small corrections})$$

where Z_D and $\dot{Z}_D$ are the Z displacement and Z velocity of the secondary ions at the detector, r_e is the radial coordinate of the point where the secondary ion is created (emission radius) and B_θ is the magnetic field produced by the plasma current at the emission radius.

When attempting to measure current density on realistic toroidal devices, two factors complicate the analysis; (1) the toroidal geometry is not amenable to an analytic solution, (2) the CF has small r and θ components in addition to the main ϕ component. The r, θ components of CF (which we will call the fringing field) can be as large as the field produced by the plasma current. If the primary beam is injected in the midplane between a pair of CF coils and there is no current flow in the

plasma then both the primary and secondary ions will remain in this plane and the trajectories reduce to a two dimensional problem. If, however, there is a plasma current it will produce a magnetic field that displaces the probing ions out of the midplane. Once the ions are displaced out of the midplace they will interact with the fringing field to produce further displacements perpendicular to the symmetry plane. Since the strength of the fringing field is a function of the distance from the symmetry plane the trajectory equations are non-linear and can be solved only by iteration.

The problem is formulated in a cartesian coordinate system where the x-y plane is a symmetry plane between a pair of CF coils. The x axis is horizontal and radial outwards from the center of the torus. The y axis is vertical. The center of the coordinates is at the center of the plasma (i.e. the center of the vacuum vessel in the x-y plane) and the Z axis is chosen to form a righthand coordinate system. The primary beam is injected in the x-y plane at x = 24.1 cm and y = 148.cm and swept across the plasma. The detector for the secondary ions is located at x = 150. cm, y = 27.5 cm. Projection of a few typical trajectories in the x-y plane is shown in Fig. II-1. Maximum Z displacement for both primary and secondary ions is small (order of 1 cm), consequently the projection trajectories determine the x-y location of the emission point to very high accuracy (the order of .01 cm). As the beam is swept across the plasma the detector "looks" along a line that is approximately given by $y = 4x$ (more accurately this line is given by $y = .008x^3 + .43x^2 + 4.7x + .2$, but for our purpose $y = 4x$ is sufficient). A parallel plate electrostatic deflection system along the secondary ion trajectories is used to force the z displacement of the secondary ions to zero at the

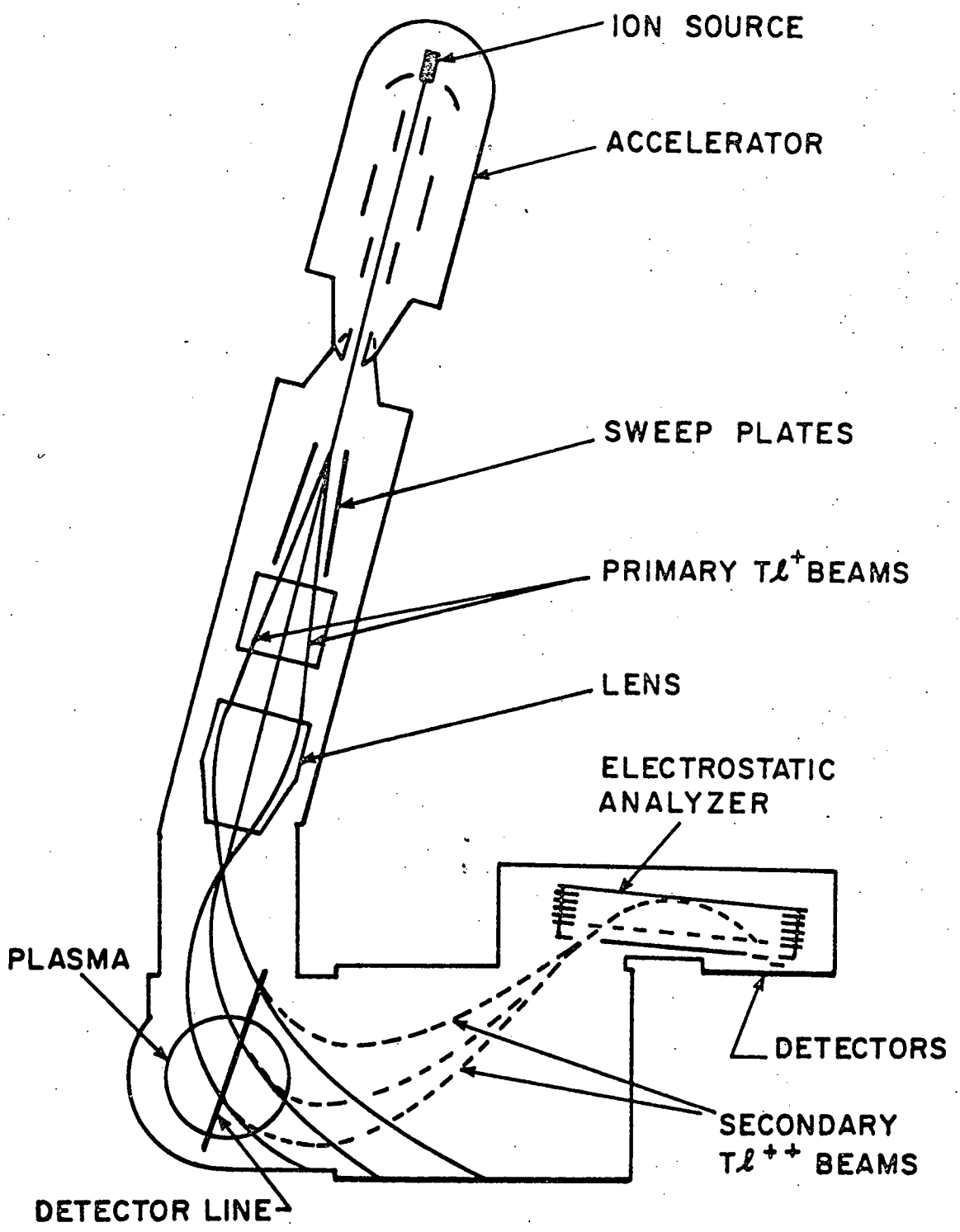

Fig. II-1 - Schematic drawing of the beam probe structure mounted on the ST Tokamak. Three primary and secondary beam paths, corresponding to maximum positive, zero and maximum negative sweep voltage, are shown.

detector. What is measured experimentally is the required voltage on the deflection system as a function of the voltage on the sweep plates of the primary ion beam. The voltage on the secondary ion deflection system is linearly related to the Z displacement that the secondary ions would have at the detector if the deflection system was not there, and the voltage on the primary sweep plates is a measure of the location of the emit point, so in effect we have a measure of Z_D vs r_e. The problem then is to extract J(r) from this measurement. Since the problem is not analytically tractable the approach taken was to calculate numerically the Z displacement at the detector for assumed current density distributions, plot Z_D vs r_e, find a correction function that will subtract out the effects produced by the fringing fields, invert the results to obtain J'(r) using cylindrical approximation and compare J'(r) with the assumed J(r) used in the trajectory calculations.

Magnetic Field Produced by the Assumed J(r)*

The magnetic field produced by a current loop can be expressed in terms of elliptic integrals. If there is a continuous distribution of current loops over a finite region of space then the total magnetic field at any point in space can be obtained by integrating the elliptic integral expression over the region occuppied by the current. To numerically calculate the orbit of a charged particle in this field requires many field evaluations and consequently an exhorbitant amount of computer time. This

*Most of this work described in this section was done under AFOSR support prior to obtaining an AEC contract and is included here in order to present a complete picture of the work.

is particularly true if you want to carry out the orbit calculations for a variety of current density distributions. To reduce the computer time requirements to a manageable magnitude it was decided to use a shell model approximation for the continuous current density distribution. Surface currents on a set of 14 nested tori having a major radius equal to the major radius of ST and minor radii that varied in 1 cm steps from 0.5 cm to 13.5 cm were used to approximate the plasma current distribution. The magnetic field at 635 points in the x-y plane were calculated for unit amplitude uniformly distributed current and unit amplitude current having a cosine distribution around the minor circumference on each torus. To obtain the approximate field corresponding to a specified current distribution, the total uniform and cosine distributed current in a hollow torus bounded by $(\alpha_i - 0.5) < r < (\alpha_i + 0.5)$, where α_i is the minor radius of the i^{th} toroidal shell, is used to normalize the tabulated field values for the i^{th} shell. The 14 values for each component of the field at each tabulated point are summed to obtain the total value of each field component at that point, and the results are punched out on cards. To calculate an orbit for any assumed current distribution the Ohmic heating (OH) field at the 635 tabulated points is read in as input data and the field at any arbitrary point is obtained by interpolation.

Effects of Fringing Fields

It is quite easy to separate the effects produced by the fringing field and the OH fields with computer simulation simply by turning the fringing fields on and off in the orbit calculations. Figure II-2 shows

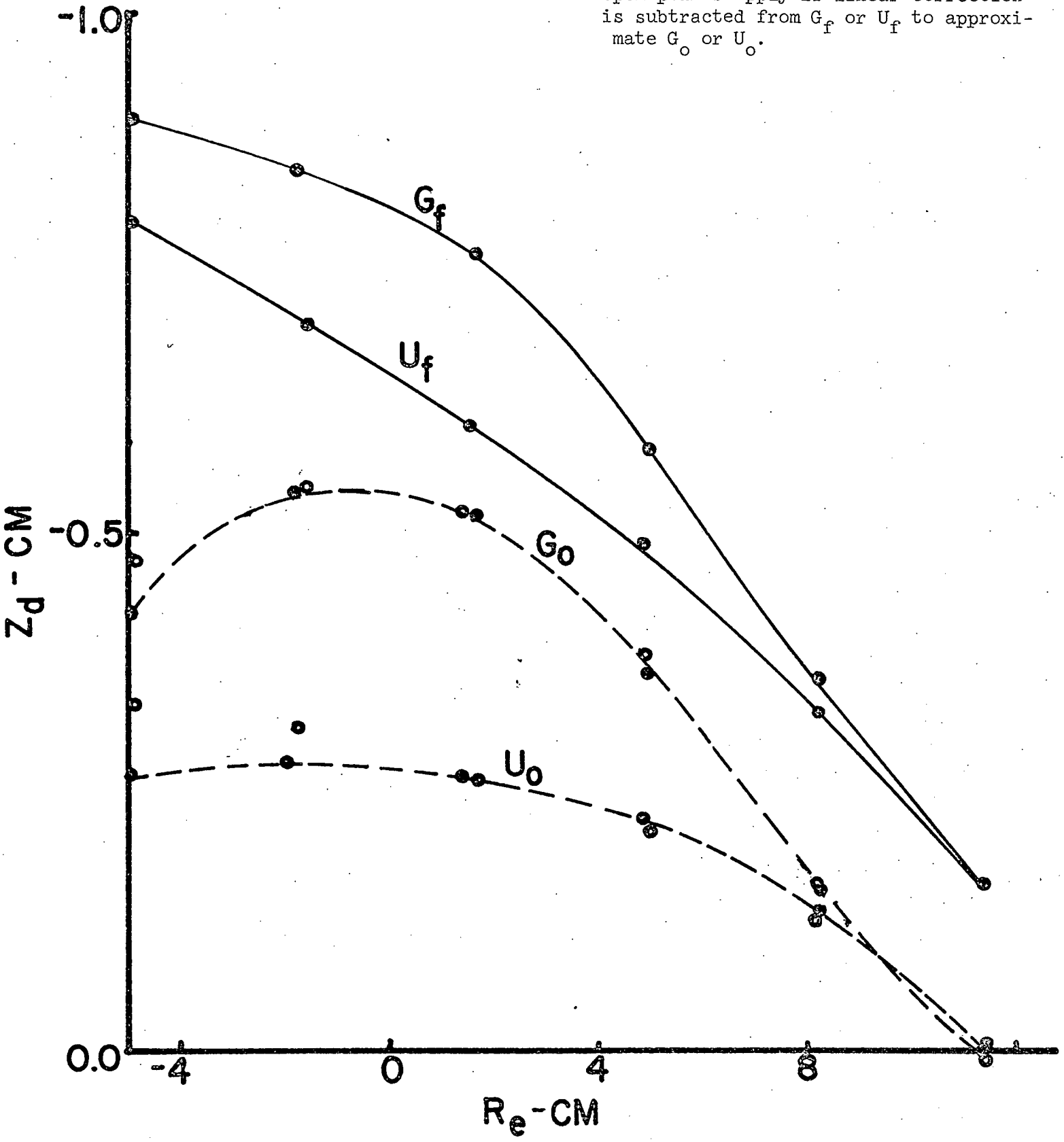

Fig. II-2 - displacement at the detector versus the minor radius of the point where the secondary ion was created. Plotted for two current distributions and two magnetic field conditions: Gaussion distribution fringing fields on and off (G_f, G_o). Uniform distribution fringing fields on and off (U_f, U_o)

the calculated Z displacement at the detector versus the minor radius of the point where the secondary ion was created for two current distributions: (1) a uniform current density and (2) a Gaussian current density with a half width of 4.5 cm. Both distributions are normalized to a total current of 17.6 K amps and cutoff at a radius of 10 cm. The gaussian distributions corresponds roughly to a $T_e^{3/2}$ conductivity for a typical operating regime where T_e has been measured by Thomson scattering.

With the fringing fields turned off the Z displacement is nearly symmetric about the origin for both current distributions. This suggests that toroidal corrections are not important and that an analysis based on cylindrical symmetry should be sufficient. The fringing fields produce two obvious effects: (1) an effective rotation of the base line and (2) a compression of the Z displacement. Our problem is to understand the cause of these two effects and see if there is an first order universal correction function independent of the current density that can be used in the data reduction to remove these effects.

In the symmetry plane (Z = 0) the fringing fields are zero and from Maxwell's equations it can be shown that the fringing field increases linearly with Z near Z = 0. The fringing fields have their maximum amplitude in the region between the ID and OD of the CF coils and the direction of the fringing fields will be primarily towards the magnetic axis of the torus (i.e. along the minor radius). Figure II-3 is a plot of Z vs r for three secondary ions emitted from 3 different points on the detector line (r is the position of the secondary ion in the coordinate system used for the calculation, $r = (x^2 + y^2)^{1/2}$). Note that the Z displacement in the region between ID and OD of the CF coils is nearly the same for all three

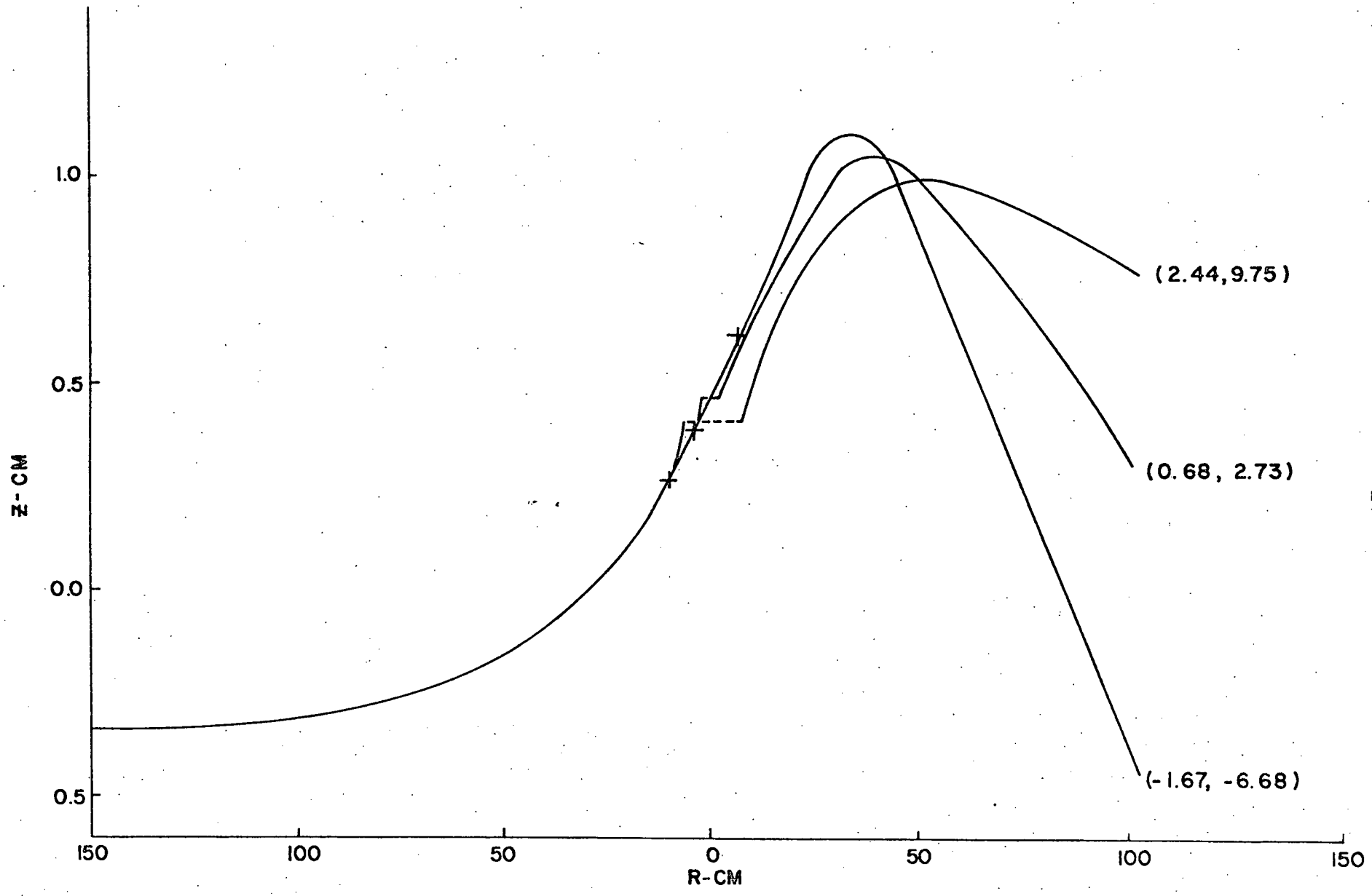

Fig. II-3 - Z displacement of the primary and secondary ions for 40 kA uniformly distributed plasma current as a function of the projection radius in the x-y symmetry plane. The coordinates along side the secondary ion orbits are the (x, y) values of the emission point. The short horizontal gaps near R = 0 occur because the particular orbits shown do not pass through the center of the plasma.

trajectroies -- i.e. - Z/Z is small in this region. Since the magnitude of the fringing field is proportional to Z, all three trajectories should sample roughly the same magnitude field. The uppermost secondary ion trajectory is almost parallel to r in the ID-OD region and as you move from one trajectory to the next the angle between the trajectory and r increases monotonically. This suggests that all the secondary ions see more or less the same magnitude of fringing field but that the angle between the ion velocity and the field direction increases monotonically with creation position along the detector line -- i.e. with sweep voltage. Furthermore, it suggests that this increase in angle between v and B is responsible for the effective rotation of the Z_D versus r_e plots shown in Figure II-2. If this is true then it should be possible to change this effective rotation by changing the average Z displacement of the secondary ions in the ID-OD region. In fact it should be possible to reduce the average Z displacement to zero in this region by tilting the injected beam. For Figure II-3 the primary beam was injected in the Z = 0 plane with ϕ, the angle between the injected velocity and Z axis, equal to 90°. This produced an averaged Z displacement in the ID-OD region of the order of 1 cm. Figure II-4 shows Z_D vs r_e for the gaussian current distribution with the fringing field on for injection angles, ϕ, of 90°, 89.9° and 89.8°. It is obvious the change in ϕ changes the effective rotation of Z_D vs r_e and that by injecting at an angle of 89.8° the effective rotation can be reduced to zero. This confirms the proposed cause of the effective rotation and provides a sensitive measure of the injection angle.

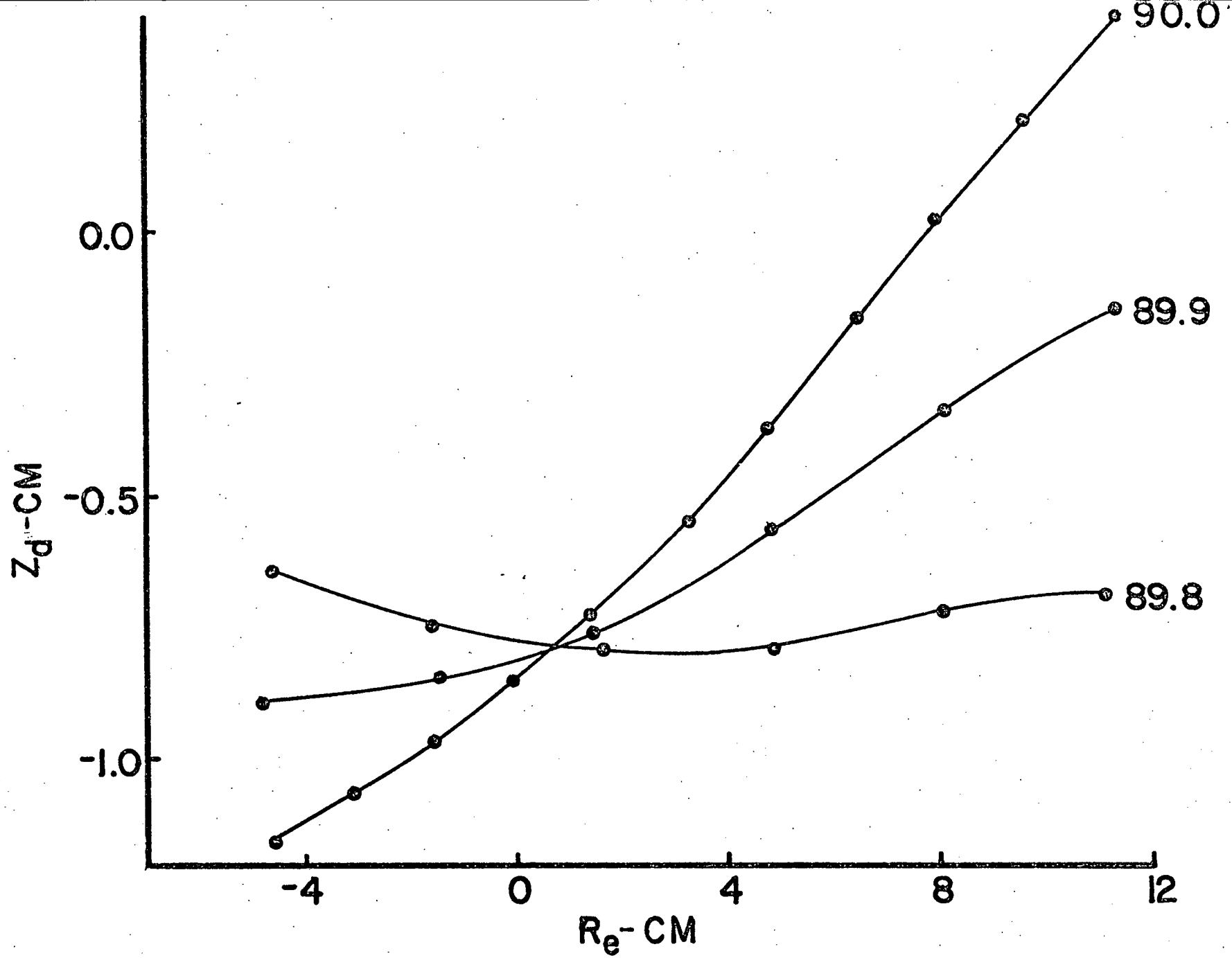

Fig. II-4 - displacement at the detector versus the minor radius of the point where the secondary was created plotted for the gaussian current distribution with fringing fields on for injection angles, ϕ, of 90°, 89.9°, 89.8°

The compression of the Z_D displacement is also due to the variation of the magnitude of the fringing field with Z. The fringing field act to reduce the Z displacement and since they vary in intensity with Z, the greater the Z displacement the greater the effect of the fringing fields. In other words the fringing fields tend to focus the Z displacement somewhere in the region of the detector (detailed calculations of Z vs r show that the fringing fields do not produce a clear focal point but they do cause a convergence of the secondary ion trajectories in the Z direction). Hopefully this focusing can be represented by a simple demagnification of the Z displacement, independent, to first order, of the current density distribution.

Combining both the rotation and demagnification, we try a trial correction function of the form

$$Z_I = M\,(Z_M - \alpha\, r_e - \beta) \qquad \text{II-1}$$

where Z_I is the Z displacement at the detector due to the OH currents, Z_M is the measured Z displacement, r_e is the emission radius (taken as negative if y_e is negative) and M, α and β are constants, independent of the current density distribution, that are to be evaluated by fitting the calculated Z_M with the fringing fields on to the calculate Z_I with the fringing fields off. Evaluating α, β and M for the gaussian current distribution with injection angle ϕ equal to 90^o, yields

$$\alpha = 0.7$$

$$\beta = 0.27$$

$$M = 1.4$$

Applying these same constants to the uniform current density calculations with ϕ equal to 90° and comparing the results with the fringing fields turned off yields the results shown in Figure II-2, comparing the curves with the open points. The results indicated that α, β and M are indeed independent of the current density for at least the gaussian and uniform case.

Preliminary calculations for a less sharply peaked gaussian and for a delta function distribution of skin current indicated that the same constants are valid in these cases, consequently we expect that to the accuracy of present measurements and calculations they are valid for all current density distributions.

To obtain the current density from the measured Z displacements we used the cylindrical approximation and evaluate $\frac{d^2 Z_I}{d r_e^2}$. The results for the gaussian and uniform current density distribution are shown in Figure II-5. The plots show the assumed J(r) that was used in the calculation (solid curve) and the J(r) that was obtained by calculating the Z_M with the fringing fields on, evaluating Z_I according to Eq. II-1 and then using finite difference to obtain $\frac{d^2 Z_I}{d r_e^2}$. (This is shown as a series of points). Qualitatively the fit is quite good and is even quite good quantatively for the gaussian. For the uniform current density case the returned J(r) is approximately 25% too small. The primary cause of scatter in the return points is the use of finite differences to evaluate $\frac{d^2 Z_I}{d r_e^2}$ combined with the fact that only 10 secondary ion trajectories were used.

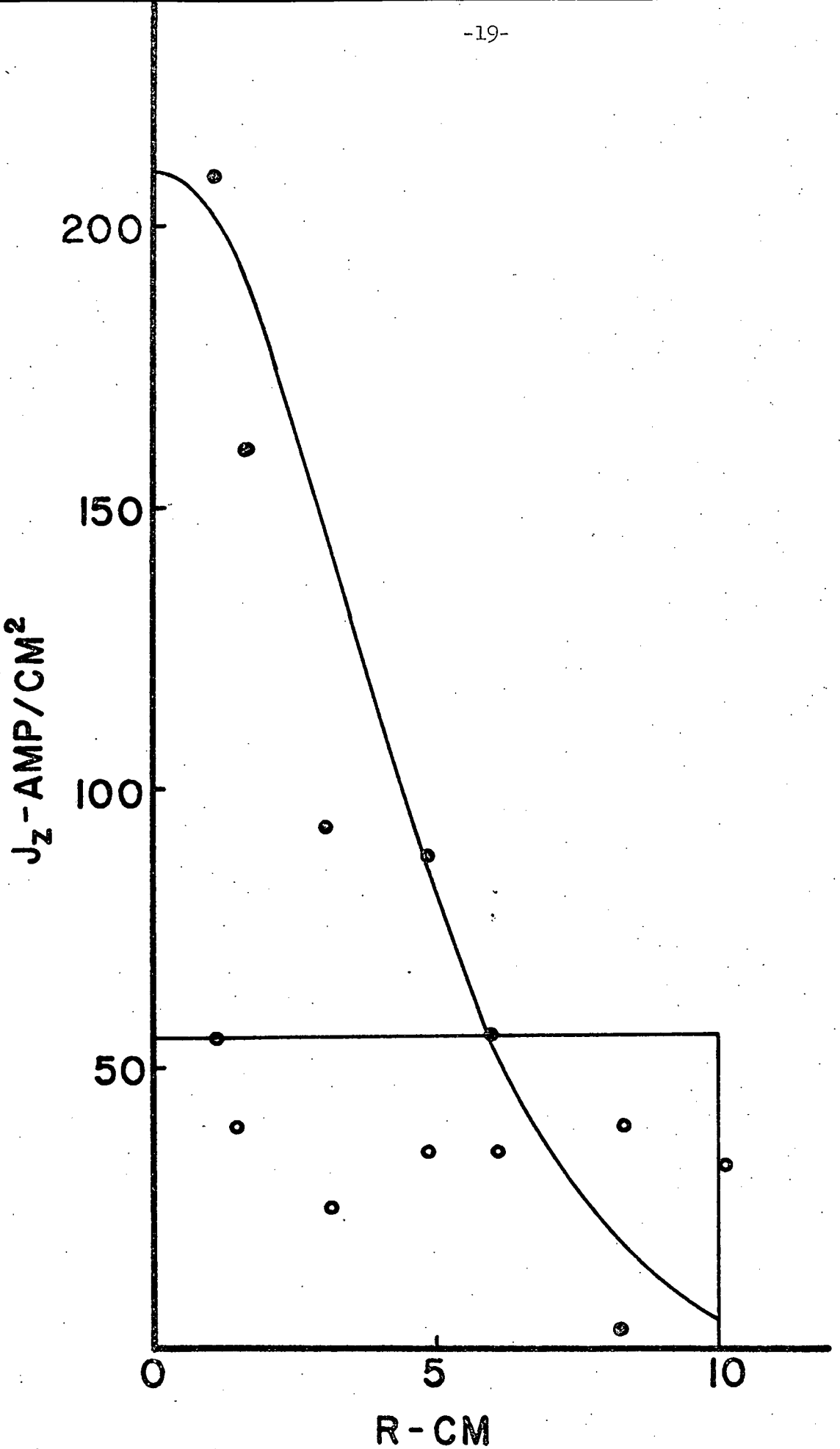

Fig. II-5 Current Density distribution versus distance from center of plasma solid curves J(r) used in calculation points, ⊙ J(r) obtained by calculating the Z_M with the fringing fields on evaluating Z_I and using finite difference to obtain $d^2 Z_I / d r_e^2$

It should be noted that in taking $\frac{d^2 Z_I}{d r_e^2}$ to obtain J(r), the arbitrary constants α and β drop out and M enters only as a normalizing factor. So the rotation of Z_M vs R_e by the fringing fields does not enter into the analysis of the experimental data and the demagnification does not effect the shape of J(r) but only its magnitude. The present analysis indicates that equation II-1 is a universal correction factor, independent of the current density distribution, to be applied in the data analysis. The accuracy of the evaluation of the constants in eqn. II-1 will not affect the shape of the J(r) results, but could effect the magnitude. This is very encouraging and provides greater cofidence in the ability of measuring J(r) with the ion beam probe. More detailed analysis of the fringing fields will undoubtedly produce higher order corrections that do depend on the current density distribution but these effects can be handled by an iteration procedure that appears certain to converge.

A potential source of error in the computer experiments is the use of toroidal shells to approximate the continuous current density distribution. The uniform current density calculation is particularly sensitive to this problem since the current on the various shells increases like r dr, consequently there is a very large current on the outer shell. Small accumulative errors in evaluating the total current on the shell and the field produced by this current can lead to substantial errors in the returned J(r). This probably accounts for the low value of the returned J(r) for this case.

Future plans call for calculating more secondary ion trajectories to obtain a better Z_D vs r_e curves and consequently a better evaluation of

$\frac{d^2 Z_I}{d r_e^2}$. The number of toroidal shells used to approximate J(r) will also be increased. Since we are using a cylindrical approximation to obtain J(r) from Z_I we also plan to use a cylindrical approximation in calculating Z_M. For this case we can use a continuous density distribution and either analytically or numerically evaluate the OH field.

III. Preliminary Design of Beam Probe System for Doublet II

In accordance with discussions held with the plasma group at Gulf Energy and Environmental Systems, the principal constraint imposed on the preliminary design of a beam probe system for Doublet II was minimizing the required port size, particularly in the region of the E coils and the wall of the field shaper. This dictated the use of a single primary beam trajectory, rather than sweeping the beam across the plasma, and consequently limits the region of measurement to a single line through the plasma. It was decided that this line or trajectory should pass through one of the foci and that the region of observation should extend to at least one edge of the plasma and if possible to both edges.

Trajectory calculations are carried out in a rectangular coordinate system where the X axis is horizontal and the positive direction is radially out from the center of the torus, the positive Y axis is vertical upwards and the Z axis is chosen to give a right hand coordinate system. The center of the coordinate system is at the top focal point -- i.e. 63.6 cm from the center of the torus and 30 cm above the vertical mid plane. The toroidal magnetic field is taken to have only a Z component, to be uniform in the Y direction inside the toroidal coils and to fall linearly to zero over the coil thickness. In the X direction B_z is assumed to vary as 1/R (R = major toroidal radius) inside the toroidal coils and to fall linearly to zero over the coil thickness. For convenience the B_z field at the center of the coordinate system was taken as 5 K gauss and the mass of the primary ions was taken as 100 atomic mass units. The energy and incident direction of the primary beam were then varied to find an

acceptable trajectory. An acceptable trajectory is one where the primary beam passes between E coil windings and through the focal point; secondary ions are observable from both edges of the plasma and provide good spatial resolution for an accessible detector location. This determines the desired incident position and momentum for the primary beam at the E coil layer. Beam momentum can be scaled to maintain the same trajectory for any desired value of the toroidal field. For a 5 K gauss field and a probing ion with a mass of 100 amu, the design beam energy is 100 KeV.

All orbit calculations have been carried out in cylindrical approximation. This is exact if the X-Y plane is selected as a mid plane between a pair of toroidal coils and all radial and poloidal components of the field are neglected. Inclusion of the radial and poloidal components produces a Z displacement of the beam and distorts the X-Y projection of the trajectories. Once the beam is displaced out of the Z = 0 plane, the X and Y components of the toroidal field should be included in the calculation (i.e. toroidal field is in the ϕ direction not the Z direction) to determine the exact trajectory. This effect will be small (for $r/R < 1$) and will primarily effect the Z displacement and not the projected X-Y trajectories.

Initial calculations to obtain an acceptable primary beam trajectory included only the toroidal field and assumed that it had only a B_z component. The selected trajectory for the primary beam and a few secondary ion trajectories are shown in Fig. III-1. The primary starts from the E coil layer (R = 95 cm) with X, Y coordinates of (31, -30). The angle between the injection velocity and the horizontal is 34°. Trajectories for four secondary ions are also shown; starting at $\pm$ 4 cm and $\pm$ 9 cm

Figure III-1 Zero order beam trajectories (including effect of toroidal confining field only)

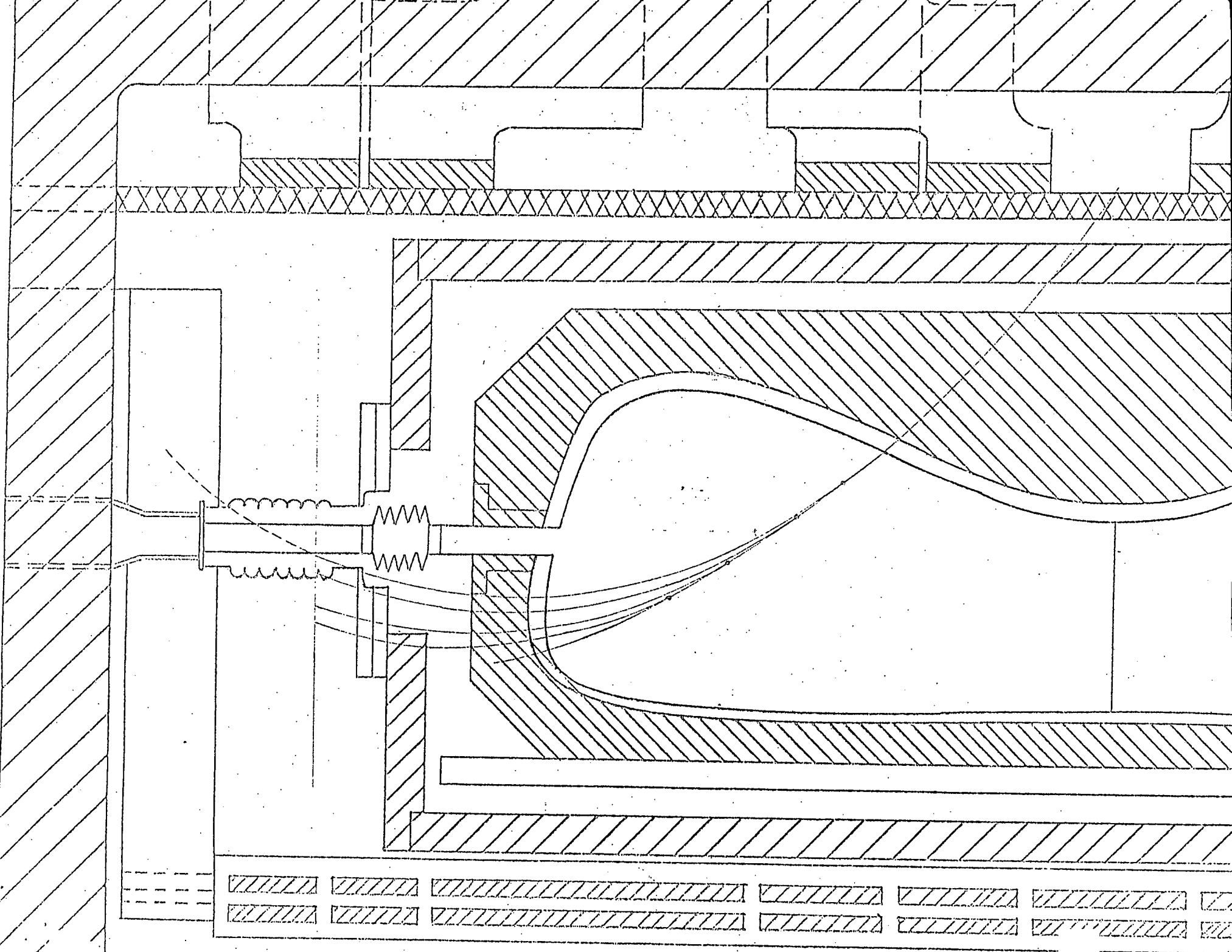

either side of the focal point (distance measured along the primary trajectory). These trajectories, which we will refer to as the zero order trajectories, serve to establish all the gross features of the ion beam probe system. They will be modified somewhat when the fields due to the E coils and the plasma currents are included in the calculation but the primary effect of these additional terms is to displace the beams out of the X-Y plane. In almost all cases the projections of the trajectories in the X-Y plane will be similar to the zero order trajectories. On the basis of these trajectories we would recommend either an array of multiple detectors or a single detector movable in the X direction (along the major radius of the torus) in the horizontal plane at Y = 50 cm. A detector at this location yields a 2 to 1 demagnification -- i.e. a 1 mm wide detector looks at 2 mm long section of primary beam path.

As can be seen from Fig. III-2 the primary beam would be injected between turns of the outside E coils and would require roughly a 2.5 cm diameter straight line port through the secondary vacuum wall, field shaper and primary vacuum wall. To observe secondary ions from one edge of the plasma to the other edge would require a port in the top of the vacuum chamber and field shaper with an X dimension of the order of 8 cm. As we will discuss in the next section the actual size required for the exit port will depend on the E coil current and on possible plasma current density distributions.

Z Displacements Produced by E-Coil and Plasma Currents

The distortion of the zero order trajectories by the fields produced by the E-coil and plasma currents were calculated in cylindrical approxi-

Figure III-2 Beam trajectories including effect of magnetic field due to E-coils. X-Y projection

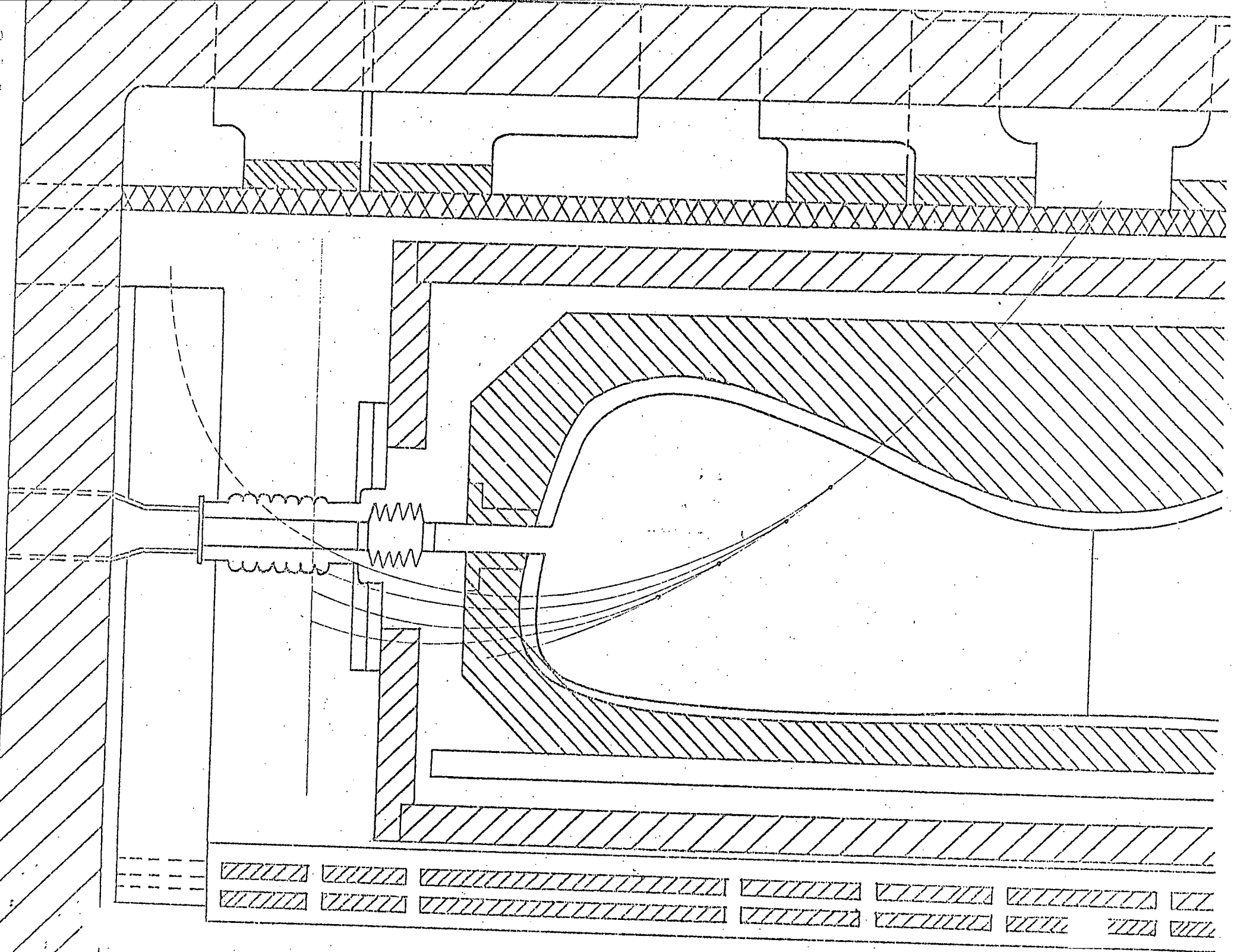

mations i.e., it was assumed that the E-coils and plasma were infinitely long cylinders and that there were equivalent cylinders on the other side of the torus that carried the return current. This is a good approximation as long as the major portion of the Z displacement is due to interaction in the region where $r < R$ $\left[r = (x^2 + y^2)^{1/2}\right]$ and R is the major toroidal radius -- (this can be put in more quantitative forms in terms of integrals along the trajectory).

Figure III-2 shows the effect of adding the E-coil current to the toroidal field -- i.e. it is assumed that there is no current flow in the plasma. Assumed operating conditions are 100 K amps in each turn of the E coil with 9 turns on the outside and 22 turns on the inside. Total ampere turns is 3100 K amps. Comparison with the zero order trajectories shows that the E coil field produces only slight distortion of the X-Y projections, however it does cause appreciable Z displacement of the beam as can be seen from Fig. III-3. Fortunately the Z displacement of the primary beam is small and would not require any enlargement of the entrance port, but the Z dispersion of the secondary ions at the primary vacuum wall and field shaper is approximately 2 cm and would necessitate an exit port this wide in order to sample all the plasma along the primary beam path.

Plasma current flow will cause additional distortion and Z displacement but this cannot be calculated explicitly without knowing the current density distribution. We can however, obtain some feeling for this effect by considering what happens for a few assumed current density distributions. The total plasma current is taken as 540 K amps which is 1/6 of the total ampere turns in the primary windings and the plasma current is taken in the same direction as the primary current. We assumed that the current

Figure III-3 Y-Z projection of beam trajectories corresponding to Figure 3

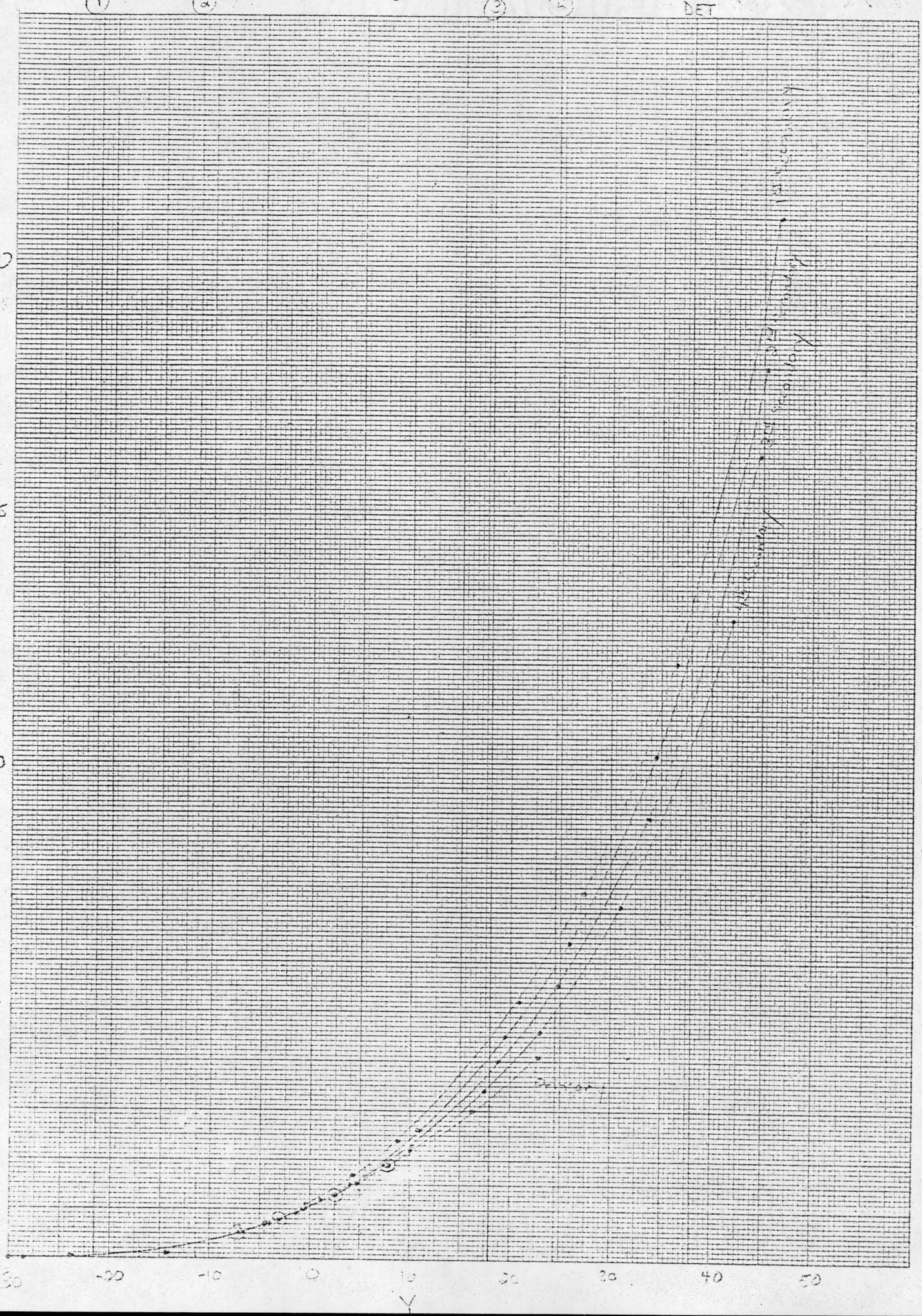

is equally divided between the upper and lower halves of the torus and considered three different cases. For each case the current density is assumed to be uniform throughout a cylinder centered on the focal point. For the first case we take the radius of the cylinder as 10 cm which approximates a uniform current distribution throughout the torus. The second case used 4 cm for the radius of the cylinder which approximates a fairly strong peaking of the current density at the focal points. For the final case we take an extreme distribution where all the plasma current is assumed to flow inside 1 cm radius cylinders centered on the focal points. Here also the calculation is done in cylindrical approximation with two cylinders on the opposite side of the torus to carry the return current. The X-Y projection of the trajectories for the three cases are shown in Figures III-4, III-6, and III-8 respectively. The Z displacement of the ions as a function of the Y coordinates of the trajectory is shown in Figures III-5, III-7, and III-9. As can be seen for the 10 cm and 4 cm radius plasma current loops the distortion of the X-Y projections is measurable but not extreme. For the 1 cm radius current filament the X-Y projections are strongly distorted, particularly for those secondaries created on the entrance side of the focal point. Figures III-5, III-7, and III-9 show that the Z displacement of the secondary ions depends on the current density distribution and although we have not established a unique relation between the Z displacement in the proposed detector plane and the current density distribution, we believe that this can be done by including a few reasonable constraints (such as the current flow is in the same direction throughout the plasma).

Figure III-4 Beam Trajectories including effect of uniform plasma current distribution within a 10 cm radius cylinder. X-Y projection

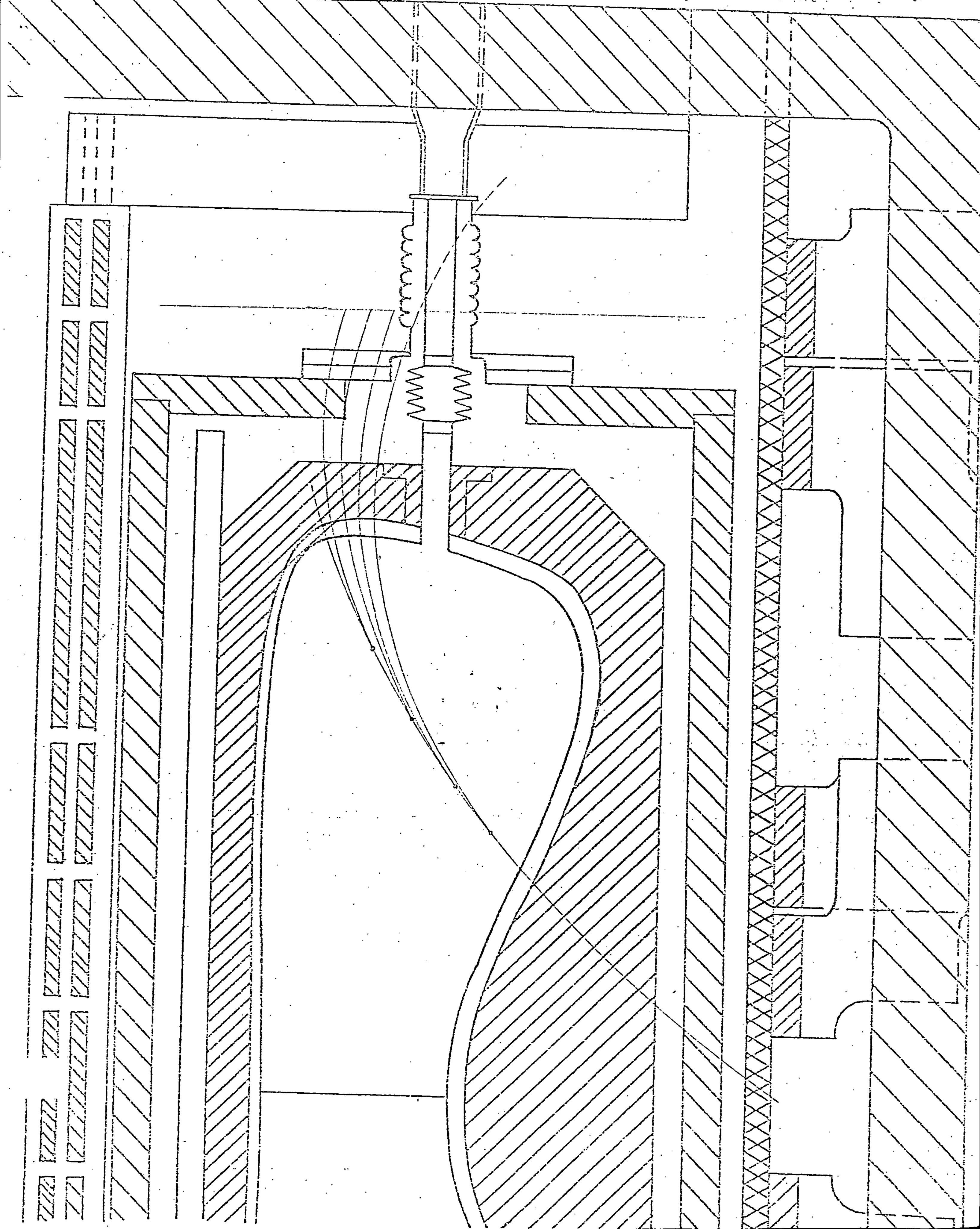

Figure III-5 Y-Z projection of beam trajectories corresponding to Figure III-4

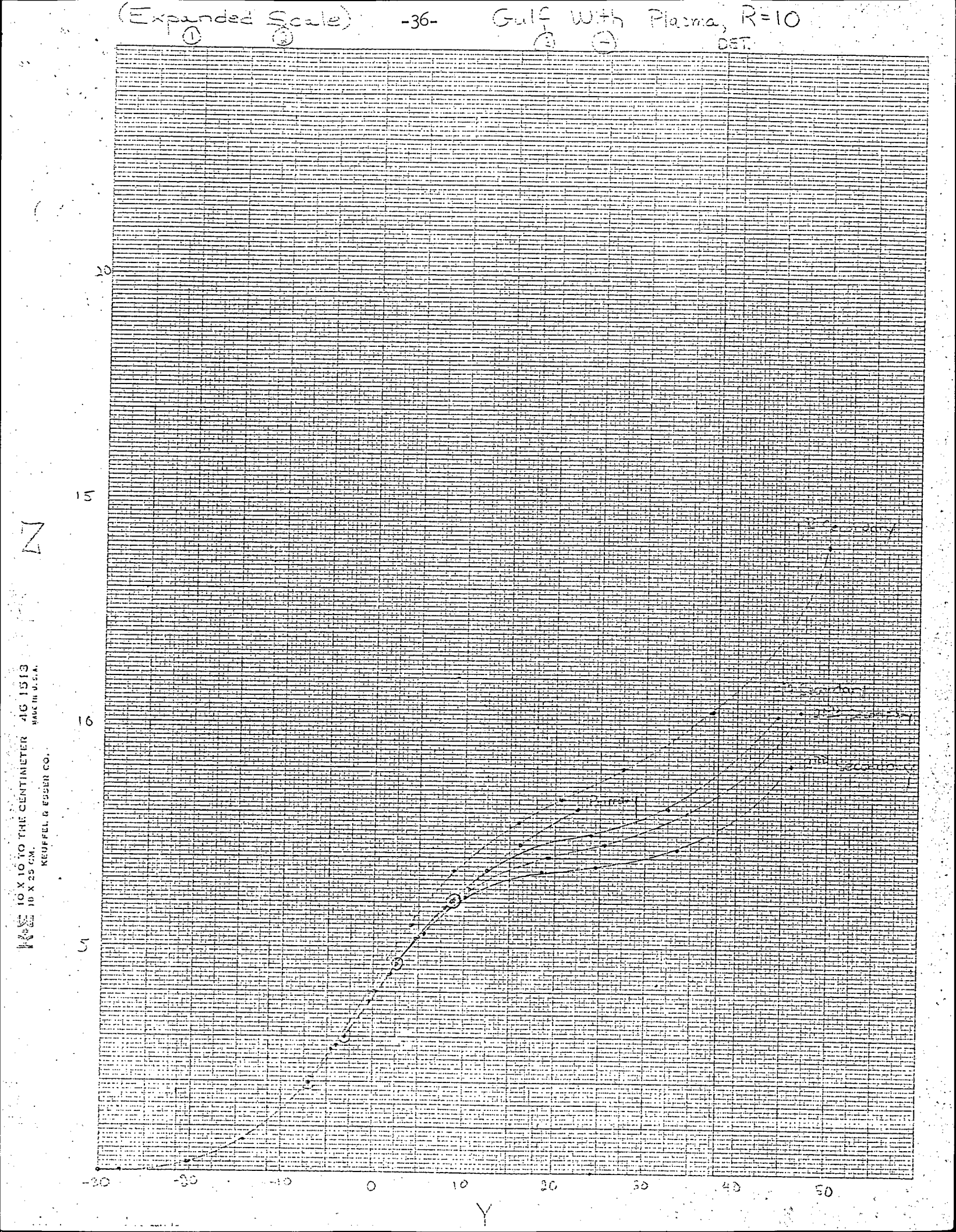

Figure III-6 Beam trajectories including effect of uniform plasma current distribution within a 4 cm radius cylinder. X-Y projection

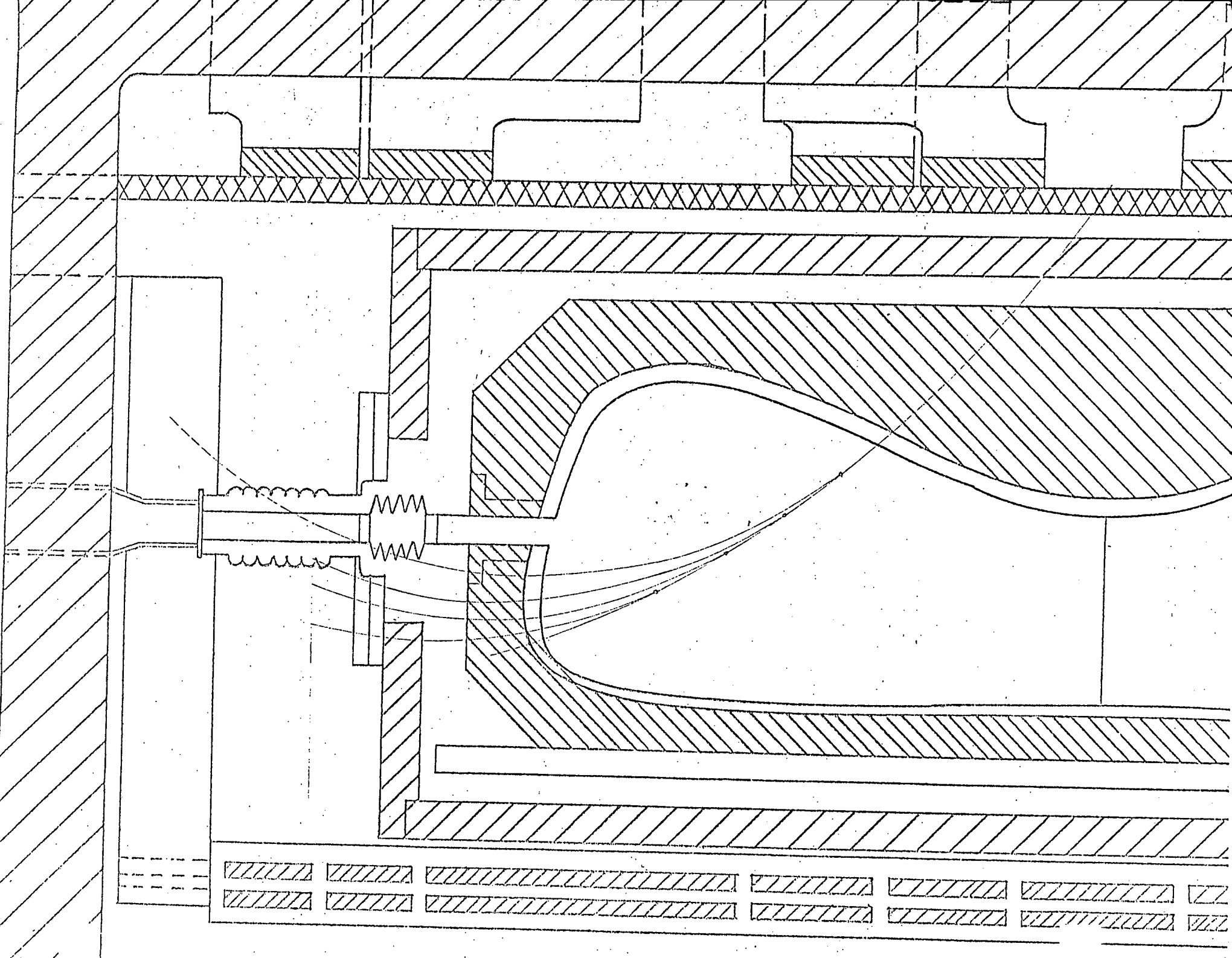

Figure III-7 Y-Z projection of beam trajectories corresponding to Figure III-6

(Expanded Scale) -40- Gulf With Plasma, R=4

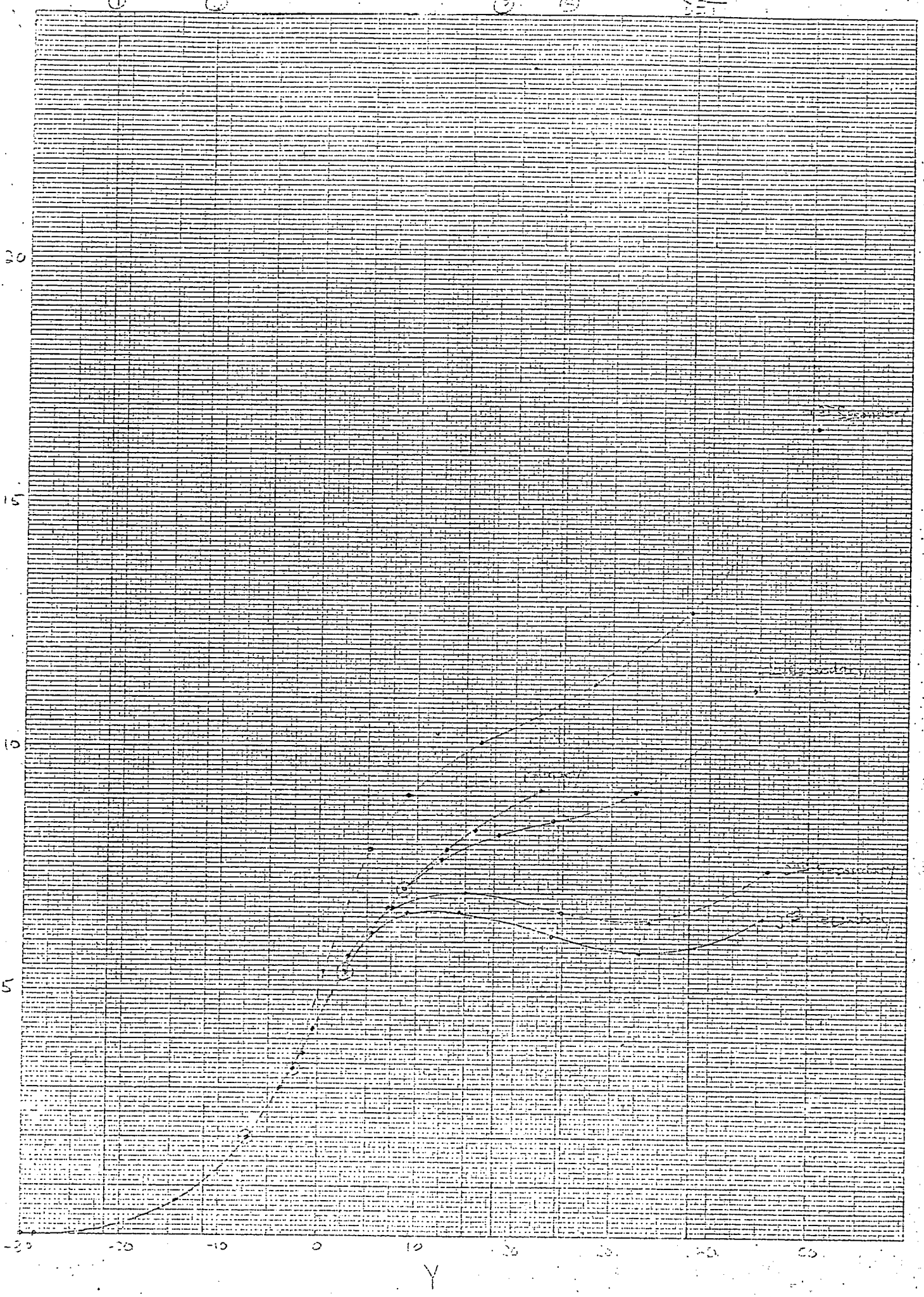

KEUFFEL & ESSER CO. MADE IN U.S.A. 10 X 10 TO THE CENTIMETER 10 X 25 CM. 46 1513

Figure III-8 Beam trajectories including effect of uniform plasma current distribution within a 1 cm radius cylinder. X-Y projection

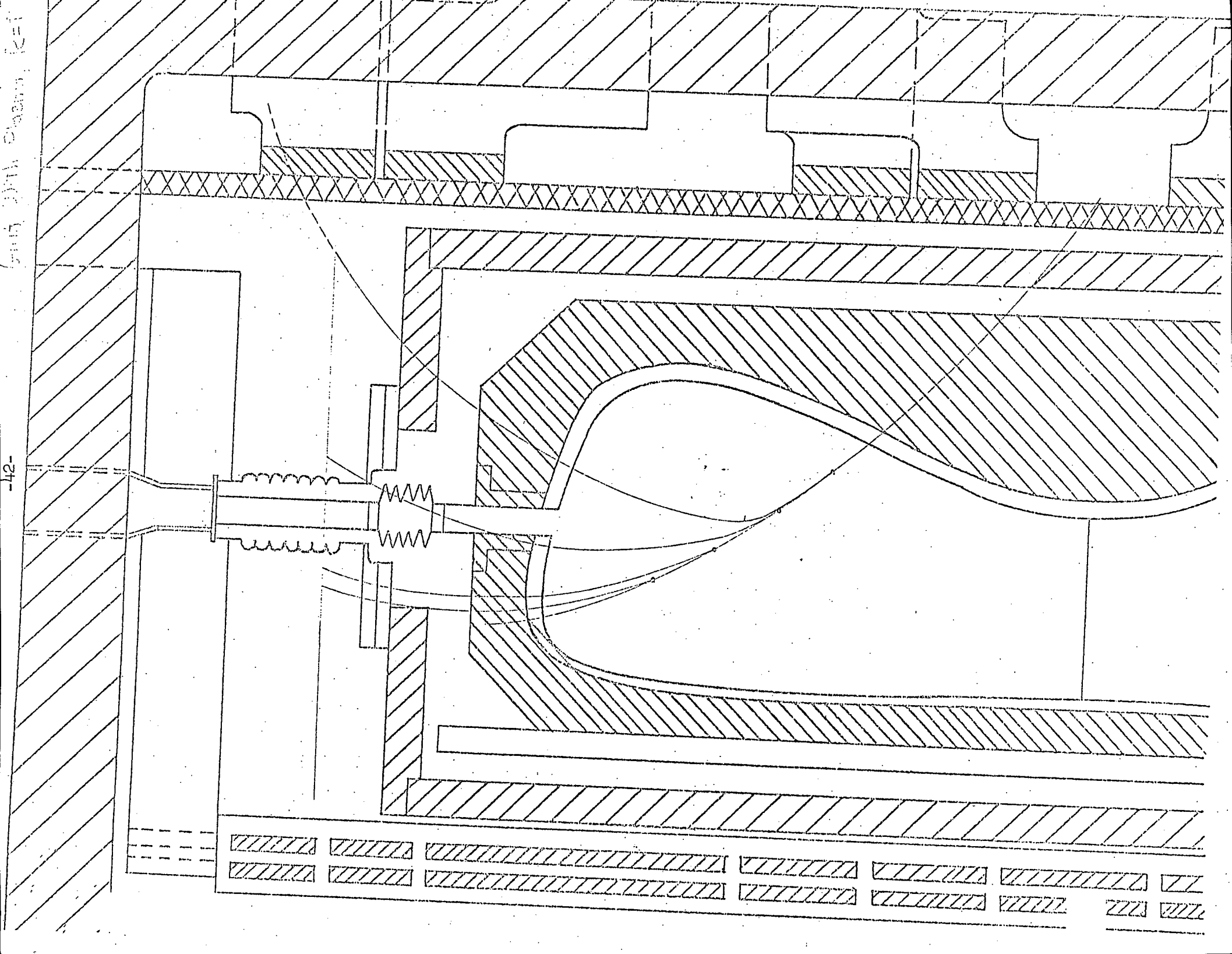

Figure III-9 Y-Z projection of beam trajectories corresponding to Figure III-8

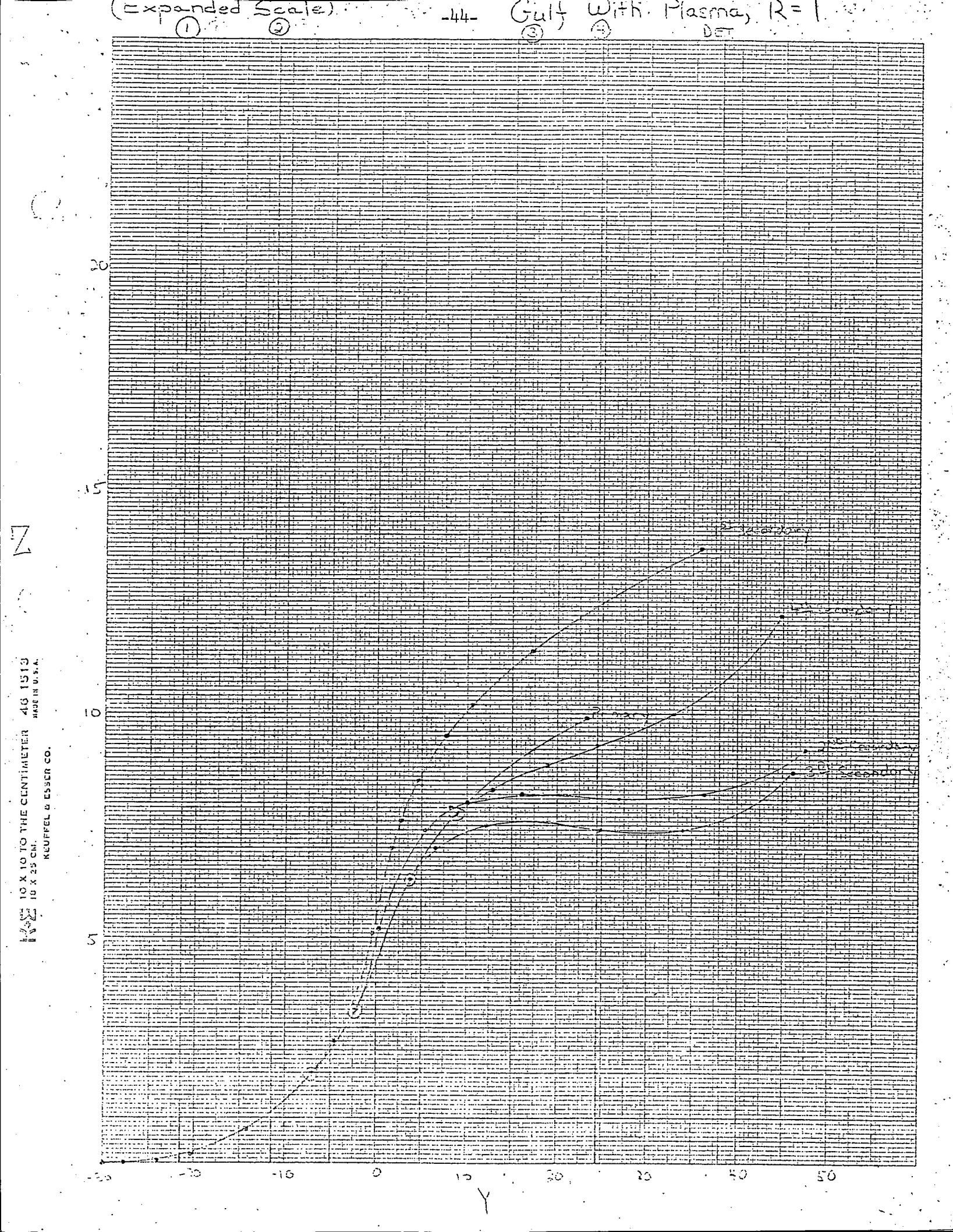

Figures III-4 - III-9 show that an exit port in the vacuum chamber and field shaper of 6 cm by 10 cm would be sufficient for an ion beam probe system. For a plasma current distribution that is very strongly peaked at the focal points some of the secondary ions created on the entrance side of the focal point will not get out the exit port but even for this extreme condition it would still be possible to obtain measurements over more than half the primary ion trajectory. If the current density is less peaked than the equivalent uniform 4 cm radius filament used in calculating the trajectories of Figs. III-6 and III-7, measurements can be made along the total length of primary ion trajectory. Obviously a large exit port would permit more measurements on extreme current density distributions.

Information Obtainable with Ion Beam Probe

It is anticipated that with a 2.5 cm diameter entrance port and a 6 cm x 10 cm exit port it would be possible to measure T_e, n and J along the entire trajectory of the primary ion. It should also be possible to measure ϕ at selected points along this trajectory but we have not included the energy analyzer in our preliminary design. Space resolution would be approximately 0.5 cm along the trajectory and approximately 0.5 cm perpendicular to the trajectory. Based on previous experience we estimate that the time resolution for a measurement at a given point could be made less than 100 μsec. With multiple detectors the complete distribution along the trajectory could be made in this time interval and the measurements would be continuous in time. How much data is accumulated in a given machine pulse would depend on the details of the data handling system.

Electron temperature measurements only provide results in the range from 0 - 200 ev. Above 200 ev the cross sections for the ionizing reactions are insensitive to T_e and the only information retrived is that T_e is greater than 200 ev. Two different ion species are required for T_e measurements. Both species can be incorporated in the same ion source but the accelerating voltage must be switched between two different values. This requires milliseconds to accomplish and therefore determines the time resolution of the T_e measurements.

Space potential measurements are complicated by choosing a detector location inside the toroidal coils but it appears possible to make use of the toroidal magnetic field in a modified Wein filter energy analyzer (i.e. use of crossed E and B fields as a velocity selector). Such a detector would be relatively large and prohibit the use of multiple detectors. Consequently ϕ measurements would be limited to one point in the plasma per machine pulse. It would be possible to follow the time history of ϕ at this preselected point during the pulse and to change location of the point under observation by moving the detector.

It is our opinion that the most severe problem that would be encountered in installing an ion beam probe on Doublet II is one of detector noise. Most of this noise would be caused by ultra-violet radiation from the plasma. The severity of this problem is unknown at the present time but we have a number of ideas on how to overcome this problem. Some possibilities include: steering the secondary ions so that the detector does not look at the plasma; thin film shielding of the detector that screens out the ultra violet but allows the beam to pass; or pulsing the

beam and using phase lock detectors. It is our opinion that this problem will require additional investigation but that it is solvable.

Present Status and Future Plans

This preliminary design study delineates the ion beam requirements, necessary port openings and the parameters that could be measured. The particular trajectories selected correspond to using a 100 Kev beam of ions having a mass of 100 amu when the center line toroidal magnetic field is 5 K gauss. In practice we would use K^+, Cs^+, Ru^+, and Tl^+ ions with the energy scaled so that they would follow the selected trajectory for any toroidal field in the range of 2 to 10 K gauss. To accommodate the beam probe system there would have to be a 2.5 cm diameter entrance port and a 6 x 10 cm exit port. This beam probe system would provide a density profile along the complete primary ion trajectory with a space resolution of approximately 0.3 cm^3, a time resolution in the range of 10 to 100 μsec and an accuracy of better than 20%. (If T_e is high, relative density measurements would be accurate to a few percent.) Measurement of the Z displacement of the secondary ions in the detector plane would provide a measure of the plasma current density distribution. It is difficult to estimate or quote an accuracy of this measurement but if, for example, the current density had cylindrical symmetry about the focal point and a radial gaussian distribution, we estimate that we could determine the half width of the gaussian to better than 20%. Space potential measurements would be limited to one (or at best a few) points along the primary trajectory during one machine pulse. Accuracy for the ϕ measurements would be 10 to 20 volts and it would be possible to follow the time evolution of

the space potential at the preselected point. If the electron temperature is below 200 ev it could be measured at all points along the primary trajectory to an accuracy of 10% to 100^{+}% depending on the value of T_e (the lower the temperature the higher the accuracy). Temperature measurements requires the use of 2 ion species which in turn requires that the accelerator voltage be switched from one value to another. This requires a time of the order of milliseconds and would set the time resolution of the T_e measurement.

If there is a decision to continue the development of an ion beam probe for Doublet II the work will proceed according to the following sequence:

1. Determine if a detector noise problem exists, find an acceptable solution if necessary.
2. Refine the trajectory calculations using more accurate magnetic field.
3. Complete the detailed design and, in collaboration with Doublet operating personnel, specify the details of the port openings and the mating connections for the beam system.
4. Construct and test the system at RPI.
5. Install and test on Doublet II.

It is estimated that this program would required from 10 to 18 months with a target time of 12 months.

IV. Preliminary Design of Beam Probe System for a Baseball Magnetic Geometry

In cooperation with the plasma physics group at the United Aircraft Research Laboratory we have undertaken a preliminary design study of an ion beam probe system for their laser produced plasma, confined in a "baseball" magnetic field. Ion trajectories in this field are much more complicated as there is no symmetry plane where the problem reduces to two dimensions. For ST and Doublet the preliminary design was begun using two dimensional trajectory in the symmetry plane which is exact when there is no plasma current. Plasma current makes the problem three dimensional, but the primary effect is to produce a Z displacement with, in general, very little distortion of the projections in the x-y symmetry plane. For the baseball geometry the trajectories are always three dimensional in just the CF field. Fortunately there is no plasma current in this system so the total field is determined by the current in the external windings (this is not true in the initial stages where $\beta > 1$ but for the time being we only consider the later stages where the field has penetrated the plasma).

Magnetic Field

In designing a beam probe for a particular device the first step is to obtain a mapping of the magnetic field. This can either be a table of experimentally measured field points or a procedure for calculating the field. Generally an experimental table that covers the full volume sampled by the beam probe is not available so it is necessary to calculate the field. This was true for the UARL baseball and we have approached the calculation of the field two ways. The first and most advanced method is

the use of a computer code furnished by UARL that provides a value for the three field components at any specified point in space. This code is a modification of a general purpose magnetic field calculation code developed at Lawrence Radiation Laboratory (UCRL Report 7744 Rev. II). The major problem with this code is that it is expensive if you have to calculate a large number of points. Consequently we do not use the code as a subroutine in the trajectory code as this requires many field evaluation. Instead, we have used the field code to generate a course table of field values which is then read in as input data for the trajectory calculations. This table provides field values on a 5 x 5 x 5 cm grid inside a 25 x 25 x 25 cm cube. The magnetic field at any point inside the cube is obtained by three dimensional quadratic interpolation and symmetry requirements. Interpolation on this coarse grid provides field values on any point that are within 10% of the values obtained with the UARL-UCRL code as long as the point in question is not near one of the planes containing the four loops that make up the baseball windings. The large variation in the fields from one side of these planes to the other leads to large inaccuracies in the interpolated field values. It turns out that linear interpolation in this region (within 5 cm of the current planes) is far more accurate and provides values that are within 30% of the UARL-UCRL code values. Checks of beam trajectories using both the interpolation field and the UARL-UCRL code field shows that the discrepancy in the final beam position is generally less than a few cms. The general shape of the trajectories is the same for both fields. Consequently the interpolation scheme provides sufficient accuracy for preliminary design studies.

We are presently developing an independent process for calculating the magnetic field by an expansion in spherical harmonics. The field intensity is expressed as the gradient of a magnetic potential

$$\beta = - \nabla \phi_m \qquad \text{(IV-I)}$$

where ϕ_m is given in terms of the magnetization[1]

$$\phi_m = - \nabla \cdot \int \frac{M}{(x - x')} \, dv' \qquad \text{(IV-II)}$$

and the magnetization is expressed as a series expansion in spherical harmonics

$$M(\theta, \phi) = \sum_{l,m} A_{lm} P_l^m \cos m \phi \qquad \text{(IV-III)}$$

Preliminary evaluation using only a few terms in the expansion indicate that the results will agree with the UARL-UCRL code results to within a few percent. It appears possible to write the field in terms of a few fixed coefficients for the spherical harmonics, in which case field evaluation will be much less expensive than the UARL-UCRL code and probably less expensive than the quadratic interpolation on tabulated field values.

Ion Trajectories

The coordinate system used for calculating the trajectories is shown in Fig. IV-1. This is a view looking towards the x-y plane for the positive

[1] Jackson, J. D. Classical Electrodynamics, J. Wiley and Sons, Inc., 1962.

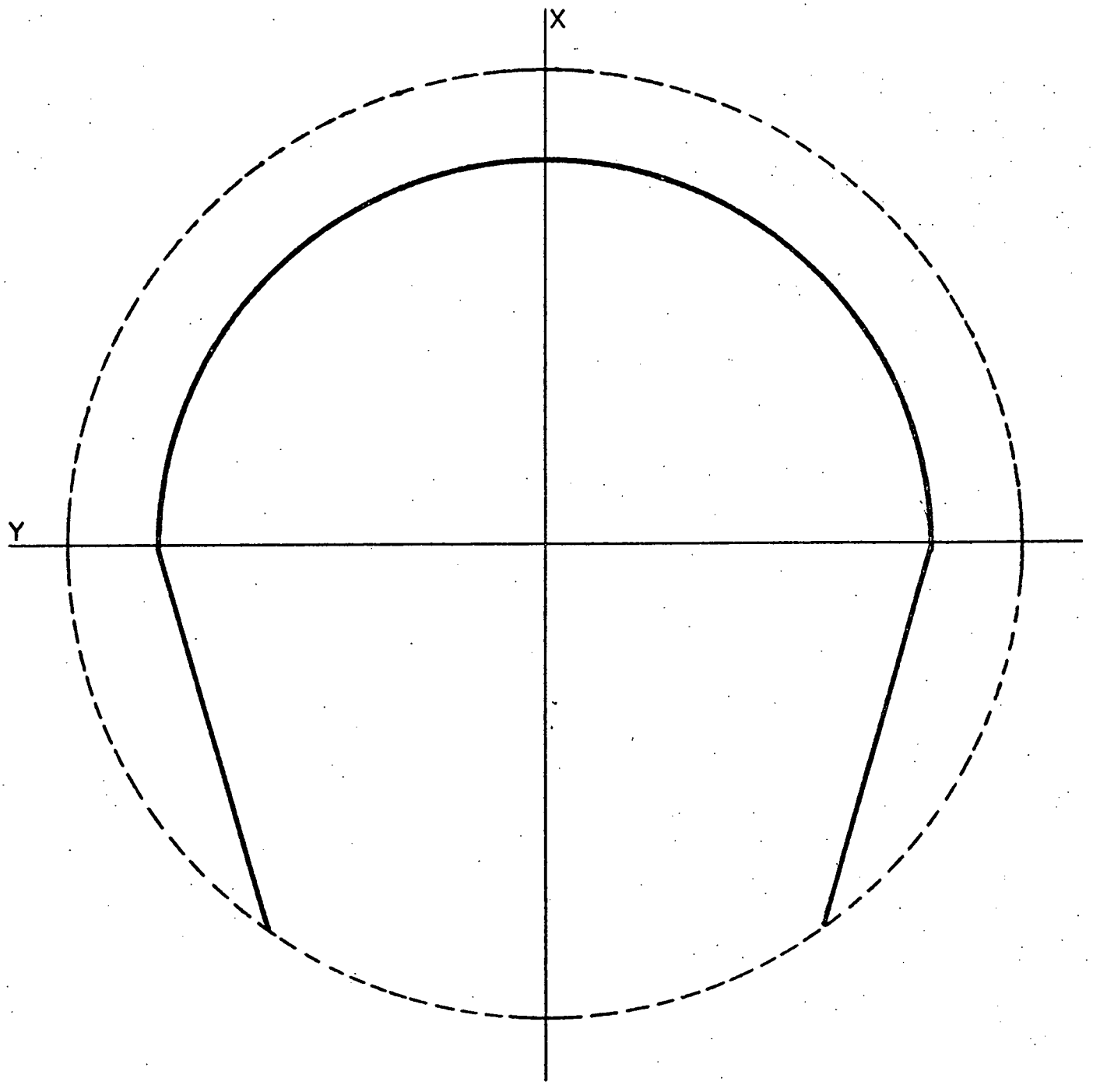

Figure IV-1 Coordinate system used for calculating trajectories. View is looking towards the x-y plane from the positive z direction.

Z direction showing the outline of the spherical surface that contains (approximately) the windings and the top view of the windings. Initially the ions were started from the center of the system in a variety of directions and the mass and energy varied to obtain some feeling for the trajectories. These calculations provided starting points outside the field for primary ion trajectories that will pass through the center of the system and allow us to make some estimates of the secondary ion trajectories. On this basis we selected momentum slaving conditions of 100 KV ions having a mass of 100 amu for center magnetic fields of 16 K gauss. The best injection conditions appear to be a starting point of x = -2.5 cm, y = 4.2 cm, z = 16.6 cm with the initial velocity in the direction $\theta = 38.5^{\circ}$, $\phi = 151^{\circ}$ where ϕ is the angle with Z axis and θ is the angle between the x-y projection and the x axis. A three dimensional projection of this trajectory and the trajectory of a few secondary ions is shown in Figure IV-2.

With this starting point and a fixed detector located at x = -6. cm, y = -2.0 - -4.0 cm, Z = -2.0 cm, then sweeping the beam in θ and ϕ will allow the plasma properties to be mapped out over a complex surface in the plasma. X-Z and Y-Z projections of the detector line and beam paths on this surface are shown in Figure IV-3 and IV-4. In general the angle between the detector line and beam path is quite large (going to 90° in some places) indicating it is possible to obtain good spatial resolution. It appears that it may be possible to sample a volume of plasma (instead of just a surface) by a combination of θ, ϕ and energy sweep.

Port requirements are not too excessive and are close to being diametrically opposite one another. This is in contrast to the toroidal

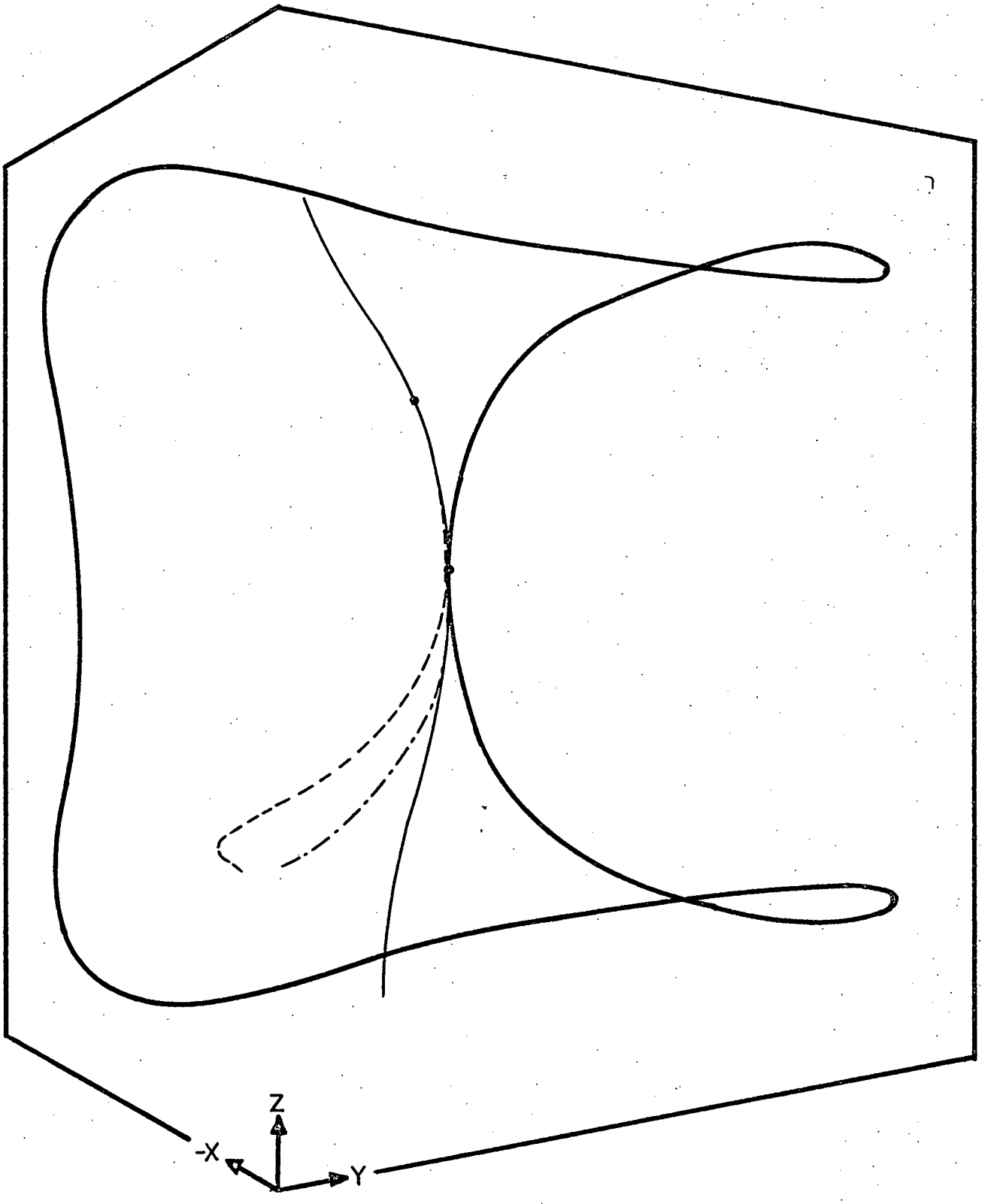

Figure IV-2 Three dimensional projection of beam trajectory, primary and two secondaries

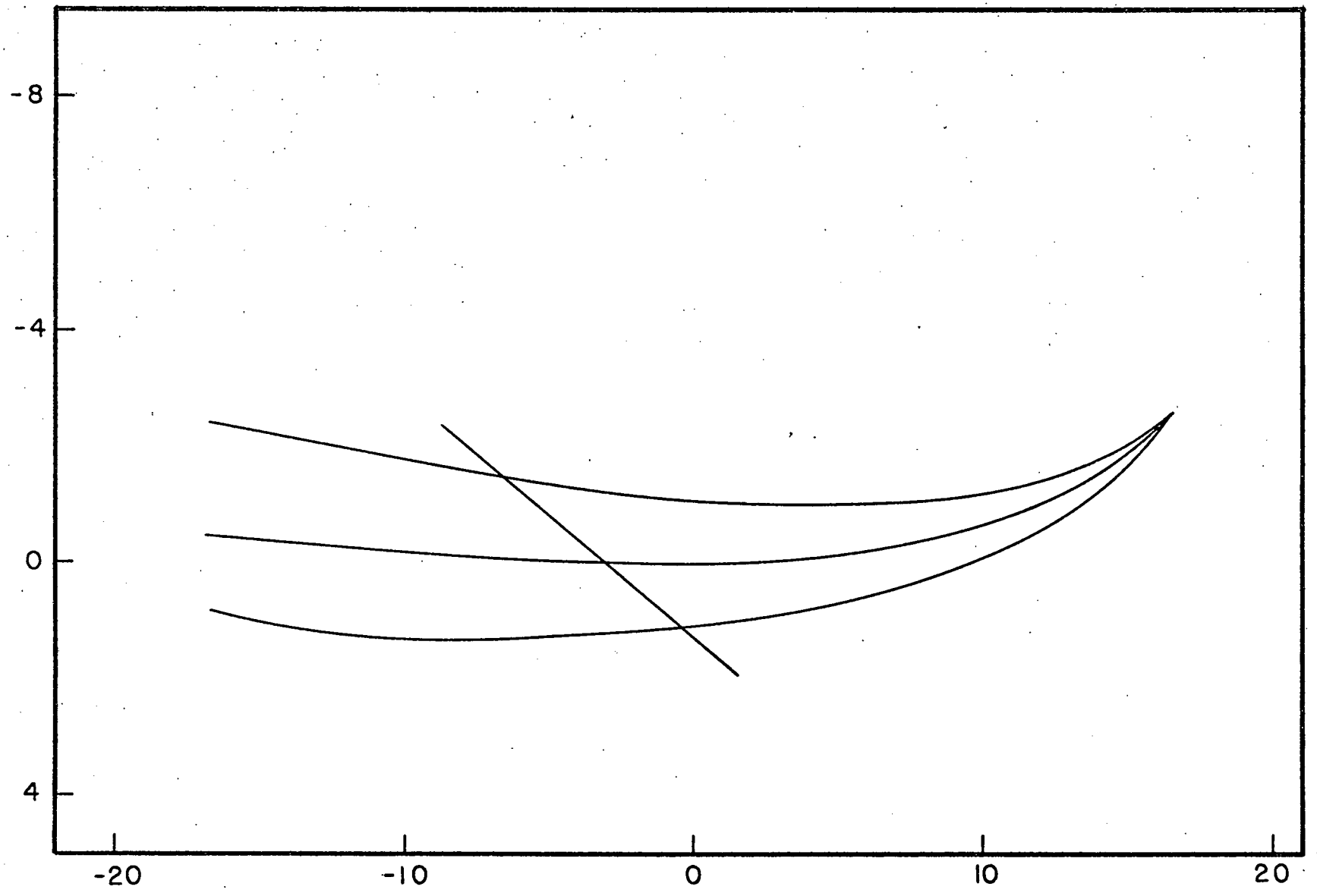

Figure IV-3 X-Z projection of detector line and beam paths

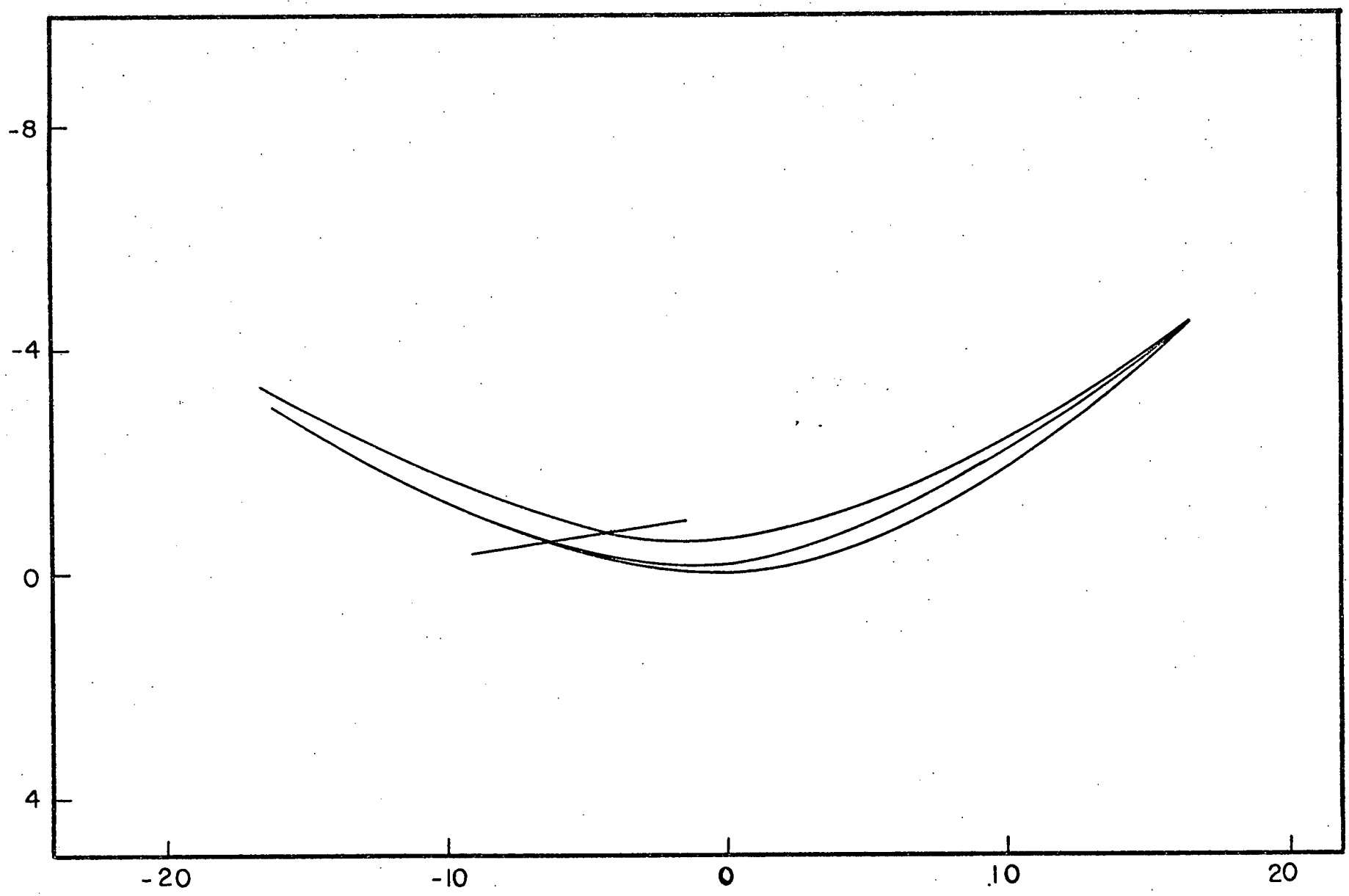

Figure IV-4 Y-Z projection of detector line and beam paths

system where the entrance and exit ports are closer to 90^{o} apart. Whether or not the desired ports are available will have to be taken up with UARL.

V. Experimental Program at RPI

The experimental part of the AEC sponsored program at RPI can be divided into two primary areas: (1) demonstrating the use of ion beam probe to measure electron temperature (2) setting up a test stand to check out and improve the ion gun, ion optics and electrostatic energy analyzer.

Measurement of T_e

The intensity of the secondary ion current for an ion beam probe system is given by

$$I_s = K I_p n_e F(T_e) \qquad \text{(V-I)}$$

where K is a constant geometrical factor, I_p is the primary ion current, n_e is the electron density at the point where the secondary ion is created and $F(T_e)$ is the probability of creating a secondary ion. $F(T_e)$ is given by the cross section for the ionizing reaction averaged over the electron velocity distribution as observed by the primary ions. This can be written as

$$F(T_e) = \frac{\langle \sigma v_e \rangle}{V_{beam}} \qquad \text{(V-II)}$$

If we take two different ion species and adjust the energy so that they have the same momentum and consequently follow the same trajectory, we can evaluate the ratio of secondary to primary current for each ion. This may be expressed as

$$\frac{I_s^1/I_p^1}{I_s^2/I_p^2} = \frac{F^1(T_e)}{F^2(T_e)} = \frac{\langle \sigma_1 v_e \rangle / V_b^1}{\langle \sigma_2 v_e \rangle / V_b^2} \qquad \text{(V-III)}$$

For a given primary beam momentum $\langle \sigma v_e \rangle / V_b$ can be plotted as a function of T_e provided the cross section is known. If we take two ion species then $F^1(T_e)/F^2(T_e)$ can be plotted as a function of T_e and by measuring the primary to secondary current ratio experimentally we have a direct measure of electron temperature.

The ion beam probe on the RPI hollow cathode discharge utilizes a beam momentum of 8.8×10^{-16} gm cm/sec. For T_e measurements we choose to use K^+ and Na^+ beams having energies of 12.7 Kev and 7.5 Kev respectively. Figure V-1 is a plot of $F^K(T_e)/F^{Na}(T_e)$ as a function of T_e for this particular choice of beam energies using cross-sections reported by Kieffer.[2]

Figure V-2 shows typical I_s/I_p data for K^+ and Na^+ beam probe measurements on the RPI hollow cathode discharge (HCD). The signals are recorded as a function of sweep voltage, which is linearly proportional to position along the detector line. The particular detector line used for these data is very nearly linear and passes through the center of the plasma. Both signals show a similar base line of 0 to 0.025 nA, which is attributed to low level beam scattering. By taking the ratio of the K^+ and Na^+ data and using the curve shown in Fig. V-1, the electron temperature can be evaluated at all points along the detector line. Once T_e is known, the density can be determined from either the K^+ or Na^+ measurements. The resulting radial profile for T_e and n_e are shown in Fig. V-3. T_e varies from 6 to 9 ev over the region r less than 1.5 cm. For r greater than 1.5 cm the

---

[2] L. J. Kieffer, Atomic Data, 1, 19 (1969).

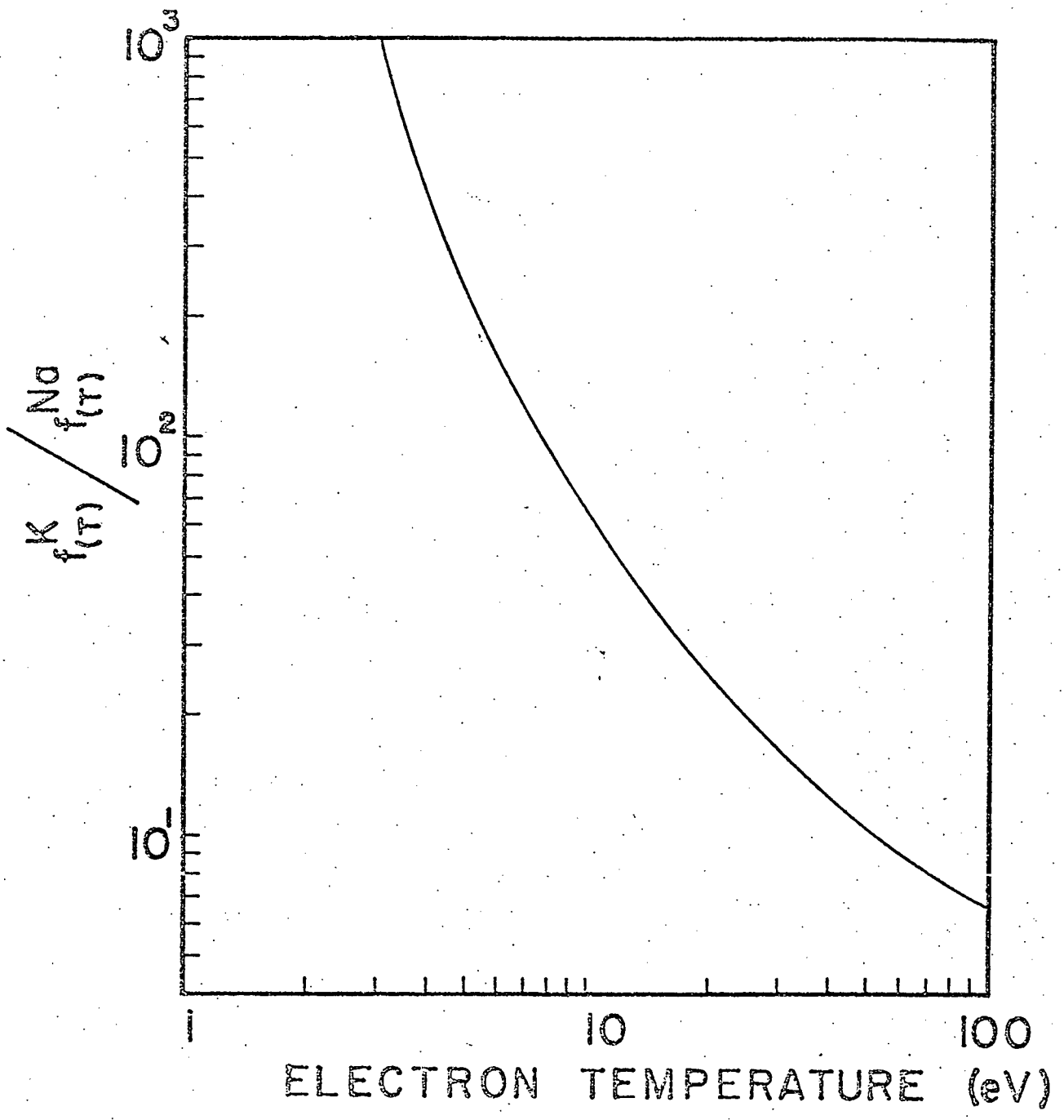

Figure V-1 Ratio of effective cross sections for potassium to sodium probing beams. The normalized secondary current ratios for two probing beams is a direct measure of $F_1(T_e)/F_2(T_e)$, resulting in direct evaluation of T_e.

Figure V-2 Recording of normalized secondary currents as a function of sweep voltage (or position in the plasma) for the sodium and potassium beams. Scale factors differ by a factor of 100. Ratio of signals at any point is a direct measurement of T_e. With T_e known, either signal can be used to determine n_e.

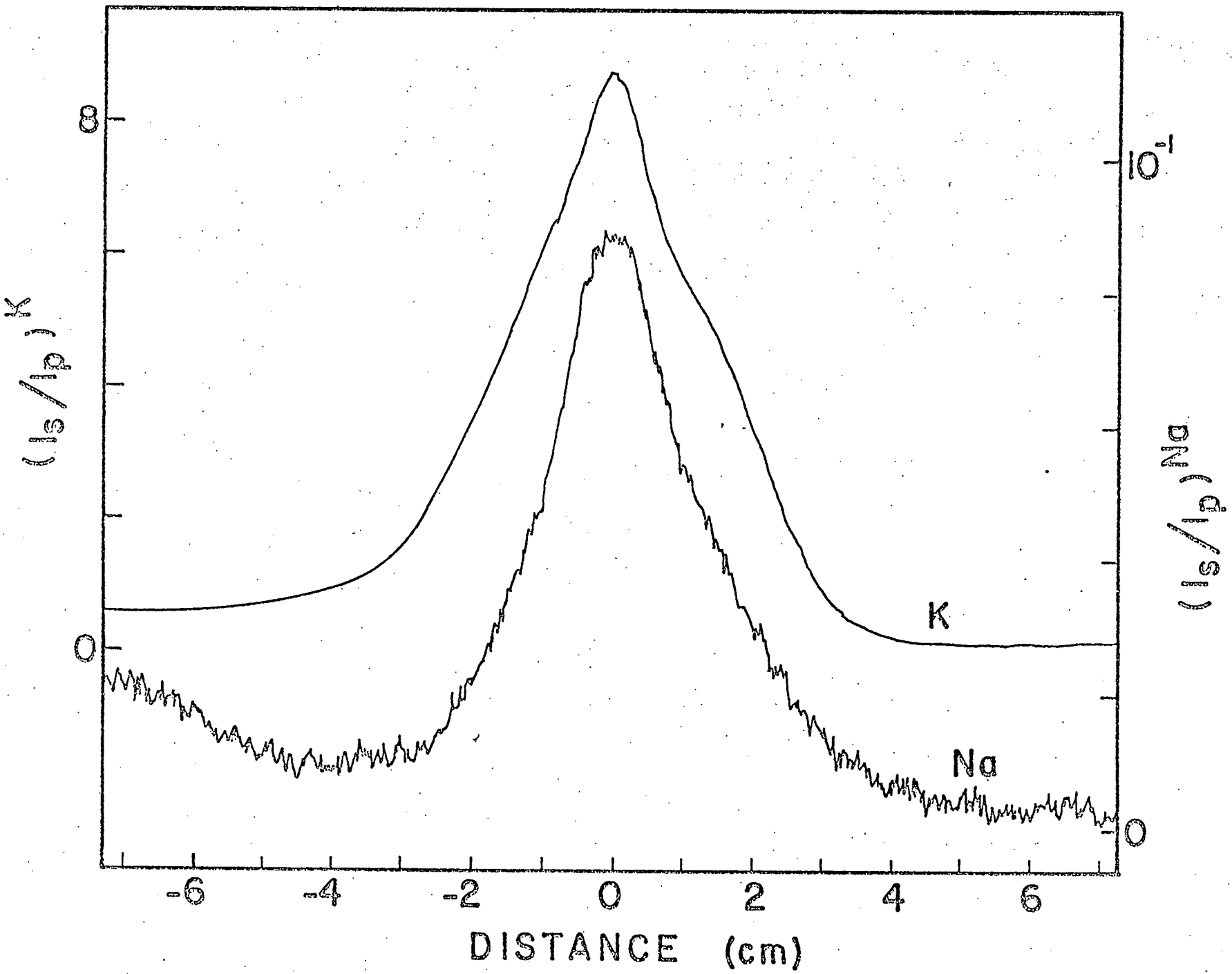

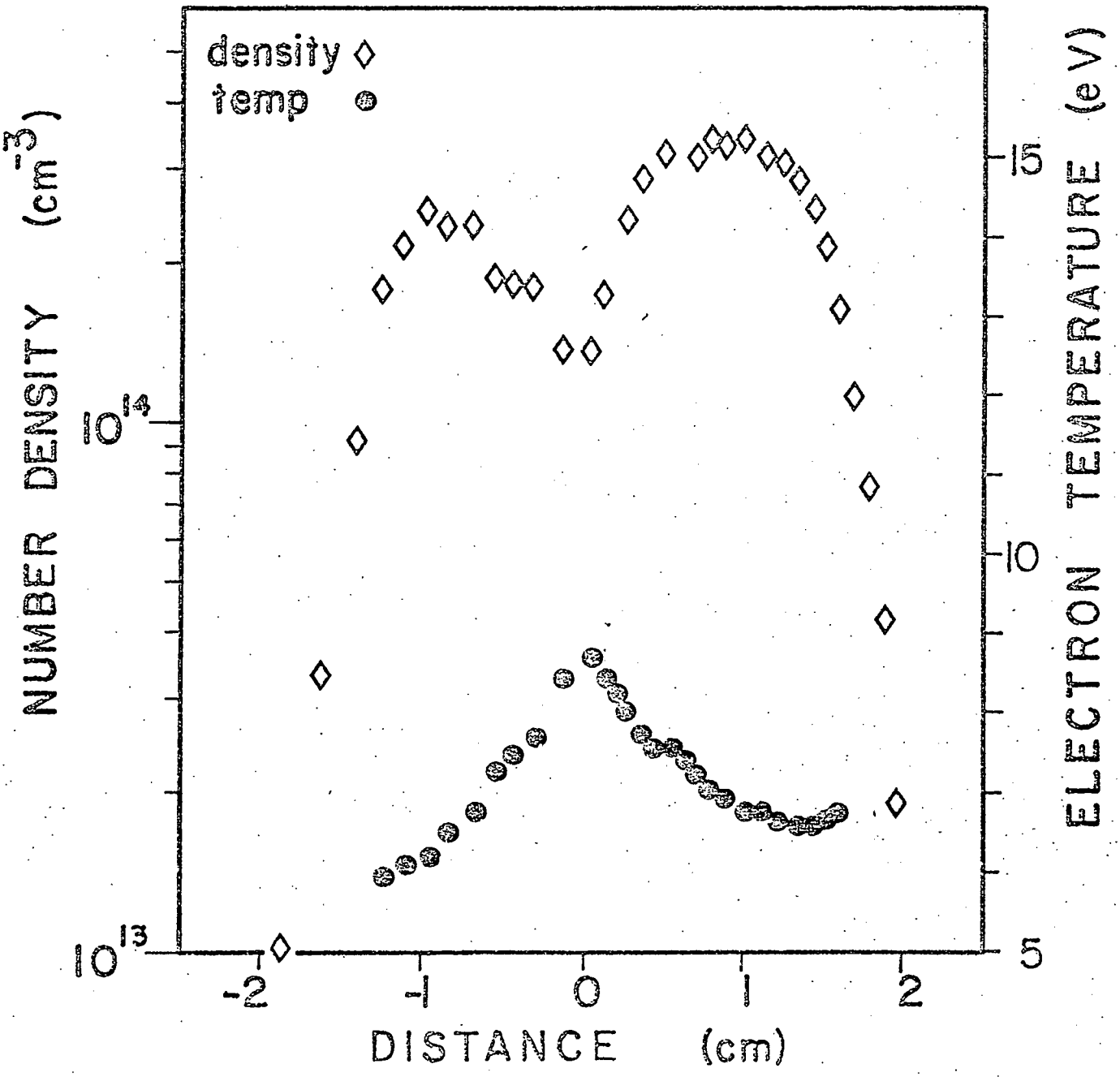

Figure V-3 Data reduced by digital analysis to yield density and temperature profiles along a detector line through the center of the plasma.

secondary ion signal is too weak to provide accurate intensity ratios for evaluation of T_e. The density profile remains essentially flat over the central region at about 3×10^{14} cm^{-3} and falls rapidly to less than 1×10^{13} cm^{-3} for $r > 1.5$ cm.

The largest source of error in the measurements is the uncertainty in the cross-section data. For the temperature range of this experiment $F(T_e)$ is a rapidly varying function and the cross-section uncertainty can only lead to small errors in T_e. However a small error in T_e (less than 1 ev) may yield an uncertainty as large as an order of magnitude in the density measurements.

The results shown in Figs. V-2 and V-3 clearly establish the ability of ion beam probing to measure T_e in the low temperature regime (less than 200 ev). It requires the use of two ion species and the present results were obtained by using two ion sources. This required that the system be shut off and brought to atmospheric pressure between measurements. However we have recently demonstrated that the two ion species can be incorporated in the same ion source. Consequently the two measurements can be obtained by simply varying the accelerator voltage. This will reduce the time resolution for the measurements to 1 millisecond or less depending on the characteristics of the accelerator power supply. Since the measurements are quasi-continuous, it should be possible to follow the time history of the electron temperature on a millisecond time scale.

Test Stand

In using ion beam probes it is necessary to determine the characteristics of the ion beam in order to evaluate the spacial resolution function.

For space potential measurements it is also necessary to determine the resolution function of the electrostatic energy analyzer. Both of these problems are best handled on a test stand set up for this specific purpose. Our test stand consists of a 4" vacuum pumping station capable of producing a base pressure of 10^{-7} torr, an ion gun and electrostatic analyzer chamber fabricated from Al and 6" diameter pyrex pipe, an ion gun and analyzer which are duplicates of the one used on the HCD system, a 20 KV power supply to drive the gun and analyzer and associated electronics to measure the response.

Initially we will use the test stand to check out the optics of the ion gun, focusing electrodes, sweep plate assembly and electrostatic analyzer of the type used for the HCD measurements. We are particularly interested in the change in ion optics when switching from one ion species to another. For a paraxial, no space charge model, the ion optics should scale linearly with accelerating voltage. However, experience on the HCD with K^+ and Na^+ beams has shown that this simple model is not accurate. The discrepancy is probably related to the difference in space charge blow-up for the two different velocity beams.

Space potential is determined from the voltage required on the electrostatic energy analyzer to bend the beam onto the exit slit. For a given incident direction of the beam at the entrance of the analyzer, the difference between the analyzer voltage and the accelerator voltage is directly proportional to the space potential where the secondary ion was created. This particular incident direction is called the design entrance angle. For a given-energy secondary ion the analyzer voltage is a function of the

entrance angle. Normally the system is set up so that secondary ions from the mid-point of the detector line enter the analyzer at the design angle, while secondaries from all other points enter at a slightly different angle. Consequently, space potential profiles must be corrected for the incident angle resolution function of the analyzer. In designing the analyzer attempts are made to minimize the variation in voltage versus incident angle (for angles near the design angle) by using entrance skimmer plates which in effect change the size and location of the entrance slit. The effectiveness of the skimmer plates is determined by computer calculations of the ion trajectories through the analyzer. Assuming that the computer model is accurate it still cannot precisely predict the resolution function for a specific analyzer since this will depend on the mechanical accuracy of the assembly and the details of the fringing electric fields. The only way to determine the resolution function for a given analyzer is to measure it. Generally this cannot be done on the plasma system since only secondary ions can enter the analyzer and their energies are determined by the unknown space potential. On the test stand the resolution function will be determined directly by measuring the analyzer voltage as a function of incident angle for the primary ion beam.

Eventually the test stand will be used for ion source lifetime measurements and to evaluate new ion source designs. It will also be used to design rapid switching of the accelerator voltage from one value to another and to test out new ion optics.

Supplementary Experimental Program at RPI

During the past year the university has furnished, at their own expense, a new 1100 square foot plasma laboratory. This laboratory was turned over to us in November 1972 and we are in the process of installing a high current, hollow cathode arc facility that was donated to RPI by Mobil Research and Development Corporation. This is the same facility on which ion beam probing was initially developed. The high current arc should be operational by September 1973. Once the high current arc is in operation the more versatile magnetic geometry used for the HCD will be available for other experiments. The current density in the high current arc is of the same magnitude as the current density in the ST Tokamak and we will attempt to make use of this for measuring current density distributions in the simpler linear geometry.

The university has also furnished funds for the construction of a 100 MW, Q switched, Nd glass laser. When this is operational we will attempt Thomson scattering measurements for comparison with the beam probe results.

An attempt to produce turbulent heating in the HCD discharge will also be made during the coming year. Dual cylindrical baffles separate the mid chamber, where the beam probe measurements are made, from the electrode regions of the HCD. A small capacitor bank will be discharged through these baffles in an attempt to produce a large current pulse in the central region. The temperature, density and space potential will be monitored with the ion beam probe.

Future plans call for looking at the characteristics of Mev heavy ion beams using an available 3 Mev Van de Graaff accelerator. The next generation plasma devices, such as the PLT, will require Mev ion beam probes and although nuclear physicists have accelerated heavy ion beams, the ion optics required for plasma beam probing are quite different and needs to be investigated.